THE SURFACE CRACK PROBLEM IN AN ORTHOTROPIC PLATE UNDER BENDING AND TENSION

by

BING-HUA WU and F. ERDOGAN

November 1986

Lehigh University
Bethlehem, PA

THE NATIONAL AERONAUTICS AND SPACE ADMINISTRATION GRANT NO. NGR-39-007-011

THE SURFACE CRACK PROBLEM IN AN ORTHOTROPIC PLATE UNDER BENDING AND TENSION

by

BING-HUA WU and F. ERDOGAN

November 1986

Lehigh University
Bethlehem, PA

THE NATIONAL AERONAUTICS AND SPACE ADMINISTRATION GRANT NO. NGR-39-007-011

Abstract

In this study the elasticity problem for an infinite orthotropic flat plate containing a series of through and part-through cracks and subjected to bending and tension loads is considered. The problem is formulated by using Reissner's plate bending theory and considering three dimensional material orthotropy. The Line-spring model developed by Rice and Levy is used to formulate the surface crack problem in which a total of nine material constants have been used. The main purpose of this study is to determine the effect of material orthotropy on the stress intensity factors, to investigate the interaction between two asymmetrically arranged collinear cracks, and to provide extensive numerical results regarding the stress intensity factors. The problem is reduced to a system of singular integral equations which is solved by using the Gauss-Chebyshev quadrature formulas. The calculated results show that the material orthotropy does have a significant effect on the stress intensity factor .

Chapter 1
Introduction

In recent years the increasing use of composite plates in many engineering structures and especially in the aero-space industry has brought up the need for more intensive stress analysis of anisotropic materials. Up to now no completely analytical solution of the related failure problems has been available due to the inherent difficulties involving the stress analysis and material characterization. In many cases the failure is attributed to the growth of cracks or crack-like flaws which exist in the structure. During the past two decades many investigators have studied the stress state in the immediate neighborhood of the crack tip since the local fracture of a structure appears to be governed mainly by this stress field. The singular behavior of the stress state near the crack-tip as characterized by the stress intensity factor depends on the magnitude of the external loads, the configuration of the body including the crack size and shape, and the material properties. Problems of a surface crack in a structural component which may locally be represented by "plate" or "shell" have long attracted the attention of investigators who have been interested in fracture mechanics. In the past few years there has been some renewed interest in the Line-spring model, (which was originally developed by Rice [1]) for solving surface crack problems in plates and shells. This interest seems to be justified because of the relatively high accuracy of the results obtained from this model (see, for example, [2], [3] and [4]). The purpose of this study is to extend the method to orthotropic elastic plates. The stress intensity factors for two orthotropic plates and one isotropic plate are extensively studied for through and part-through cracks. Here the isotropic case has been considered for the

purpose of comparison. In materials undergoing fracture it is often observed that small pre-existing cracks or cracks generated during service join together and grow into major cracks to cause final failure. Thus, theoretical analysis of the interaction of multiple cracks in the structure is quite important. Consequently, the emphasis in this study will be on the interaction of two collinear, semi-elliptic surface cracks or through cracks in an infinite plate subjected to uniform bending or tension. This problem is formulated by using Reissner's plate bending theory and considering the material orthotropy with the isotropic medium as a special case. The problem is reduced to a system of singular integral equations. The effect of material orthotropy on the stress intensity factor and the interaction between two arbitrarily arranged collinear cracks have been investigated. Rather extensive numerical results have been provided which may be useful in application.

Chapter 2
The general formulation of the problem

2.1 The governing equations for an orthotropic plate under bending and tension

In this section a brief derivation of the fundamental equations for an orthotropic plate under bending and in-plane stretching is given. The problem of bending and the problem of in-plane loading are uncoupled. The material of the plate is assumed to be orthotropic with principal axes or orthotropy parallel to the co-ordinate axes. Thus the strain-stress relations may be expressed as

$$\begin{aligned}
\epsilon_{xx} &= S_{11}\sigma_{xx} + S_{12}\sigma_{yy} + S_{13}\sigma_{zz}, \\
\epsilon_{yy} &= S_{21}\sigma_{xx} + S_{22}\sigma_{yy} + S_{23}\sigma_{zz}, \\
\epsilon_{zz} &= S_{31}\sigma_{xx} + S_{32}\sigma_{yy} + S_{33}\sigma_{zz}, \\
\epsilon_{yz} &= S_{44}\sigma_{yz}, \\
\epsilon_{xz} &= S_{55}\sigma_{xz}, \\
\epsilon_{xy} &= S_{66}\sigma_{xy},
\end{aligned} \tag{1}$$

where the quantities S_{ij} characterize elastic properties of the plate material.

2.1.1 The plate under bending

The bending problem is based on the Reissner's plate theory [5], [6]. In the isotropic case the equations are given by [7]. Consider a thin elastic plate bounded by the planes $z = \pm h/2$. The resultant forces are shown in Fig. 1, where M_{ij} and V_i $(i, j = x, y)$ are respectively the moment and transverse shear resultants.

Referring to [8], the equilibrium equations may be expressed as

$$\begin{aligned} &\frac{\partial M_x}{\partial x} + \frac{\partial M_{xy}}{\partial y} - V_x = 0, \\ &\frac{\partial M_y}{\partial y} + \frac{\partial M_{xy}}{\partial x} - V_y = 0, \\ &\frac{\partial V_x}{\partial x} + \frac{\partial V_y}{\partial y} + q = 0, \end{aligned} \tag{2}$$

and, in terms of the moment and shear resultants, the stress components are given by

$$\begin{aligned} &\sigma_{xx} = \frac{M_x z}{h^3/12}, \quad \sigma_{yy} = \frac{M_y z}{h^3/12}, \quad \sigma_{xy} = \frac{M_{xy} z}{h^3/12}, \\ &\sigma_{xz} = \frac{3V_x}{2h}\left[1 - \frac{4z^2}{h^2}\right], \quad \sigma_{yz} = \frac{3V_y}{2h}\left[1 - \frac{4z^2}{h^2}\right], \\ &\sigma_{zz} = \frac{3q}{4}\left[\frac{2z}{h} - \frac{8z^3}{3h^3} + \frac{2}{3}\right]. \end{aligned} \tag{3}$$

Also, the following relations between some average values ω, ϕ_x and ϕ_y and the displacements u_0, v_0 and ω_0 are introduced in accordance with the balance of the work done by the resultant forces on the average values and by the corresponding stresses on the actual displacements

$$\omega = \frac{3}{2h}\int_{-h/2}^{+h/2} \omega_0[1-\frac{4z^2}{h^2}]dz\,,$$

$$\phi_x = \frac{6}{h^2}\int_{-h/2}^{+h/2} u_0 \frac{z}{h/2}\,dz\,, \tag{4}$$

$$\phi_y = \frac{6}{h^2}\int_{-h/2}^{+h/2} v_0 \frac{z}{h/2}\,dz\,.$$

From (1) and the strain-displacement relations it follows that:

$$\epsilon_{xz} = \frac{\partial u_0}{\partial x} = S_{11}\sigma_{xz} + S_{12}\sigma_{yy} + S_{13}\sigma_{zz}\,,$$

$$\epsilon_{yy} = \frac{\partial v_0}{\partial y} = S_{21}\sigma_{xz} + S_{22}\sigma_{yy} + S_{23}\sigma_{zz}\,,$$

$$\epsilon_{zz} = \frac{\partial \omega_0}{\partial z} = S_{31}\sigma_{xz} + S_{32}\sigma_{yy} + S_{33}\sigma_{zz}\,,$$

$$\epsilon_{xz} = \frac{\partial u_0}{\partial z} + \frac{\partial \omega_0}{\partial x} = S_{55}\sigma_{xz}\,, \tag{5}$$

$$\epsilon_{xy} = \frac{\partial u_0}{\partial y} + \frac{\partial v_0}{\partial x} = S_{66}\sigma_{xy}\,,$$

$$\epsilon_{yz} = \frac{\partial \omega_0}{\partial y} + \frac{\partial v_0}{\partial z} = S_{44}\sigma_{yz}\,.$$

If we now solve (5) for σ_{ij}, $(i, j = x, y, z)$, substitute into (3), integrate in z and use (4) we obtain:

$$M_x = \frac{h^3}{12}[S_{22}S_{11} - S_{12}S_{12}]^{-1}[(S_{22}\frac{\partial \phi_x}{\partial x} - S_{12}\frac{\partial \phi_y}{\partial y}) + (S_{12}S_{23} - S_{22}S_{13})\frac{6q}{5h}],$$

$$M_y = \frac{h^3}{12}[S_{22}S_{11} - S_{12}S_{12}]^{-1}[(S_{11}\frac{\partial \phi_y}{\partial y} - S_{21}\frac{\partial \phi_x}{\partial x}) + (S_{21}S_{13} - S_{23}S_{11})\frac{6q}{5h}],$$

$$M_{xy} = \frac{h^3}{12}(S_{66})^{-1}(\frac{\partial \phi_x}{\partial y} + \frac{\partial \phi_y}{\partial x}), \tag{6}$$

$$\phi_x = -\frac{\partial \omega}{\partial x} + S_{55}\frac{6V_x}{5h},$$

$$\phi_y = -\frac{\partial \omega}{\partial y} + S_{44}\frac{6V_y}{5h}.$$

Technically, equations (2) and (6) would give the complete formulation of the problem, the eight equations accounting for the eight variables, M_x, M_y, M_{xy}, V_x, V_y, ϕ_x, ϕ_y and ω. Eliminating first, ϕ_x and ϕ_y then M_x, M_y and M_{xy} and assuming $q=0$, we obtain the system of equations governing the small deflection of elastic orthotropic plates as follows:

$$V_{x,x} + V_{y,y} = 0,$$

$$V_x + A_1 V_{x,xx} + A_2 V_{x,yy} - A_3 \omega_{,xxx} - A_4 \omega_{,yyx} = 0, \tag{7}$$

$$V_y + A_5 V_{y,xx} + A_6 V_{y,yy} - A_7 \omega_{,xxy} - A_8 \omega_{,yyy} = 0,$$

where the coefficients A_i are constants defined in Appendix 1. The remaining unknowns can be obtained from

$$\phi_x = -\omega_{,x} + \frac{6S_{55}}{5h}V_x,$$

$$\phi_y = -\omega_{,y} + \frac{6S_{44}}{5h}V_y, \tag{8}$$

$$M_x = -\frac{h^3}{12\kappa}(S_{22}\omega_{,xx} - S_{12}\omega_{,yy}) + \frac{h^2}{10\kappa}(S_{22}S_{55} + S_{12}S_{44})V_{x,x},$$

$$M_y = -\frac{h^3}{12\kappa}(S_{11}\omega_{,yy} - S_{12}\omega_{,xx}) + \frac{h^2}{10\kappa}(S_{11}S_{44} + S_{12}S_{55})V_{y,y},$$

$$M_{xy} = -\frac{h^3}{6S_{66}}\omega_{,xy} + \frac{h^2}{10S_{66}}(S_{55}V_{x,y} + S_{44}V_{y,x}),$$

where $\kappa = S_{11}S_{22} - S_{12}S_{12}$. (9)

Note that since the basic system of equation (7) is sixth order, three conditions must be prescribed on the boundary of the plate.

Following [8], to simplify this bending problem a stress function $F(x,y)$ is introduced as follows:

$$\omega = F_{,y} + A_1F_{,xxy} + A_2F_{,yyy},$$

$$V_x = A_3F_{,xxxy} + A_4F_{,xyyy}, \tag{10}$$

$$V_y = -A_3F_{,xxxx} - A_4F_{,xxyy},$$

then, equations (7) are identically satisfied provided the stress function $F(x,y)$ satisfies the following equation:

$$B_1\frac{\partial^4 F}{\partial x^4}+B_2\frac{\partial^4 F}{\partial x^2\partial y^2}+B_3\frac{\partial^4 F}{\partial y^4}+B_4\frac{\partial^6 F}{\partial x^6}$$

$$+B_5\frac{\partial^6 F}{\partial x^4\partial y^2}+B_6\frac{\partial^6 F}{\partial x^2\partial y^4}+B_7\frac{\partial^6 F}{\partial y^6}=0\,, \tag{11}$$

where B_i are known constants defined in Appendix 1.

Equation (11) is called the fundamental equation. It is essentially a special case of that given in [8].

2.1.2 In-plane stretching problem

Begining with the usual plane stress assumption

$$\sigma_{zz}=\sigma_{zx}=\sigma_{zy}=0\,, \tag{12}$$

we define the Airy stress function $\Phi(x,y)$ as follows:

$$\sigma_{xx}=\frac{\partial^2\Phi}{\partial y^2}\quad,\quad \sigma_{yy}=\frac{\partial^2\Phi}{\partial x^2}\quad,\quad \sigma_{xy}=-\frac{\partial^2\Phi}{\partial y\partial x}\,.$$

Along with the stress-strain relation (1), the compatibility condition for an orthotropic plate may be expressed as:

$$\frac{\partial^4\Phi}{\partial x^4}+2C_1\frac{\partial^4\Phi}{\partial x^2\partial y^2}+C_2{}^2\frac{\partial^4\Phi}{\partial y^4}=0\,, \tag{13}$$

$$\text{where}\qquad C_1=\frac{S_{66}}{2S_{22}}+\frac{S_{12}}{S_{22}}\,,\quad C_2=\left(\frac{S_{11}}{S_{22}}\right)^{1/2}\,. \tag{14}$$

The fourth order differential equation (13) is subject to two conditions on the plate boundary.

As we know, the solutions satisfying equation (13) yield the following characteristic equation

$$m^4+2C_1m^2+C_2{}^2=0\,. \tag{13.1}$$

The roots of (13.1) are

$$m_1 = q_1 + i\,q_2$$

$$m_2 = q_3 + i\,q_4 \qquad (13.2)$$

$$m_3 = -m_1 \quad , \quad m_4 = -m_2$$

Where m_1 and m_2 are both real or complex conjugates. The material is defined as type 1 when both roots are real and as type 2 when they are complex conjugates.

Equations (11) and (13) give the governing equations for an orthotropic plate subjected to bending and in-plane streching.

2.2 Infinite plate containing a series of collinear cracks

2.2.1 The orthotropic plate under bending

Consider now an infinite plate containing a series of collinear through cracks which are along the y axis. This problem will be solved by using Fourier transforms. It will be assumed throughout this study that through a proper superposition, the original crack problem has been reduced to a perturbation problem in which self-equilibrating force and moment resultants acting on the crack surfaces are the only nonzero external loads. One may note that since the corresponding through crack problem is uncoupled through the governing equations as well as the boundary conditions, the in-plane loading and bending problems can be solved independently.

For the function $F(x,y)$ defined by (11) we introduce the following Fourier transformations:

$$f(x,\alpha) = \int_{-\infty}^{+\infty} F(x,y)\, e^{i\alpha y}\, dy\,, \tag{15a}$$

$$F(x,y) = \frac{1}{2\pi}\int_{-\infty}^{+\infty} f(x,\alpha)\, e^{-i\alpha y}\, dy\,. \tag{15b}$$

Substituting (15b) into (11) one obtains a sixth-order ordinary linear differential equation in f. Looking for a solution in the form:

$$f(x,\alpha) = R(\alpha)e^{mx}\,, \tag{16}$$

the charcteristic equation of the problem is found to be

$$B_4 m^6 + (B_1 - \alpha^2 B_5)\, m^4 - (\alpha^2 B_2 - \alpha^4 B_6)\, m^2 + (\alpha^4 B_3 - \alpha^6 B_7) = 0\,. \tag{17}$$

It should be emphasized here that the roots of (17) are in general complex and are functions of α.

After solving (17) let the roots be ordered such that

$$R_e(m_j) < 0, \qquad (j=1,\ 2,\ 3)\,, \qquad m_{j+3} = -m_j\,. \tag{18}$$

The solution $f(x,\alpha)$, satisfying the regularity condition at $x = \pm\infty$, may then be expressed as :

$$\begin{aligned} f(x,\alpha) &= \sum_{j=1}^{3} R_j(\alpha) e^{m_j x}\,, \qquad for \qquad (x > 0)\,, \\ &= \sum_{j=4}^{6} R_{j(\alpha)} e^{m_j x}\,, \qquad for \qquad (x < 0)\,. \end{aligned} \tag{19}$$

Because of the assumed symmetry with respect to yz plane in loading and

geometry, the transverse shear and moment resultants must satisfy the following symmetry conditions:

$$V_x(x,y) = -V_x(-x,y), \qquad V_y(x,y) = V_y(-x,y),$$

$$M_x(x,y) = M_x(-x,y), \qquad M_y(x,y) = M_y(-x,y),$$

$$M_{xy}(x,y) = -M_{xy}(-x,y). \tag{20}$$

It is therefore sufficient to consider one half of the plate only. Thus for example for $x > 0$ we find

$$F(x,y) = \frac{1}{2\pi}\int_{-\infty}^{\infty}\sum_{j=1}^{3} R_j(\alpha)e^{m_j x}e^{-i\alpha y}d\alpha, \qquad (x > 0). \tag{21}$$

Substituting from (21) into (10) and using (8) the relevant components of moment and transverse shear resultants and rotation may be expressed as follows:

$$M_{xy} = \frac{1}{2\pi}\int_{-\infty}^{\infty}\sum_{j=1}^{3} \Gamma_{xy}(\alpha)R_j(\alpha)e^{m_j x}e^{-iy\alpha}\,d\alpha, \tag{22}$$

$$\Gamma_{xy}(\alpha) = \left[\frac{h^3}{6S_{66}}m_j + \left(\frac{h^3}{6S_{66}}A_1 - \frac{h^2}{10S_{66}}S_{55}A_3\right)(m_j)^3 + \frac{h^2}{10S_{66}}S_{44}A_4 m_j^3\right]\alpha^2,$$
$$+\left[-\frac{h^3}{6S_{66}}A_2 + \frac{h^2}{10S_{66}}S_{55}A_4\right]m_j\alpha^4 - \frac{h^2}{10S_{66}}S_{44}A_3(m_j)^5,$$

$$M_x = \frac{h^3}{12\kappa}\frac{i}{2\pi}\int_{-\infty}^{\infty}\sum_{j=1}^{3}\Gamma_{xx}(\alpha)R_j(\alpha)e^{m_j x}e^{-iy\alpha}\,d\alpha, \tag{23}$$

$$\begin{aligned}\Gamma_{xx}(\alpha) = [\,&S_{22}(m_j)^2 + S_{22}A_1(m_j)^4 - \frac{6}{5h}(S_{22}S_{55} + S_{12}S_{44})A_3(m_j)^4]\alpha \\ &- [S_{22}A_2(m_j)^2 - S_{12} - S_{12}A_1(m_j)^2 - \frac{6}{5h}(S_{22}S_{55} \\ &+ S_{12}S_{44})A_4(m_j)^2]\alpha^3 - S_{12}A_2\alpha^5,\end{aligned}$$

$$V_x = \frac{i}{2\pi}\int_{-\infty}^{+\infty}\sum_{j=1}^{3}[-A_3(m_j)^3\alpha + A_4(m_j)\alpha^3]R_j(\alpha)e^{m_j x}e^{-iy\alpha}\,d\alpha, \tag{24}$$

$$\phi_{x,y} = \frac{1}{2\pi}\int_{-\infty}^{\infty}\sum_{j=1}^{3}\Gamma_{xx}(\alpha)\,R_j(\alpha)e^{m_j x}e^{-iy\alpha}\,d\alpha, \tag{25}$$

$$\Gamma_{xx}(\alpha) = [\,m_j + (A_1 - \frac{6}{5}\frac{S_{55}}{h}A_3)m_j^3]\,\alpha^2 - [A_2 - \frac{6}{5}\frac{S_{55}}{h}A_4]\,m_j\alpha^4,$$

where R_1, R_2 and R_3 are unknown functions of α and are given in Appendix 2.

In addition to the regularity condition at infinity, the bending problem must be solved under the following boundary conditions:

$$M_{xy}(x,0) = 0,$$

$$V_y(x,0) = 0, \qquad -\infty < x < \infty, \tag{26}$$

$$M_x(0,y) = p_1(y), \qquad y \in L,$$

$$\phi_x(0,y) = 0, \qquad y \in L', \tag{27}$$

where $(L+L') = (-\infty,+\infty)$, L refers to a system of collinear cracks and is finite and $p_1(y)$ is a known function . By using the homogeneous conditions (26), two of the three unknown functions R_j can be eliminated. The third one is then obtained from the mixed boundary conditions (27).

The problem may be reduced to an integral equation for a new unknown function G_1 defined by

$$\frac{\partial}{\partial y}\phi_x(0,y) = G_1(y), \qquad -\infty < y < +\infty. \tag{28}$$

Thus, from(27) by noting that $G_1(y) = 0$ on $y \in L'$ and by using (23) and (25) the first equation of (27) may be expressed in the following form:

$$\lim_{x \to 0} \int_L G_1(t)dt \int_{-\infty}^{+\infty} H(\alpha,x)e^{i\alpha(t-y)}d\alpha = p_1(y), \qquad (y \in L). \tag{29}$$

The possible singularity of the kernels in (29) at $y=t$ would be due to the behavior of $H(\alpha,x)$ as $\alpha \to \pm\infty$. For the purpose of examining the singular behavior of the kernels in (29) and for extracting the singular parts, the asymptotic behavior of m_j, as $|\alpha| \to \infty$ is needed. Thus, from (17) it can be shown that for large values of $|\alpha|$ we have

$$m_1 \approx a_1|\alpha|, \qquad m_4 = -m_1,$$

$$m_2 \approx (a_2 + ib_2)|\alpha|, \qquad m_5 = -m_2,$$

$$m_3 \approx (a_2 - ib_2)|\alpha|, \qquad m_6 = -m_3, \tag{30}$$

where a_i and b_i are material constants.

Using now the relations (30) and separating the asymptotic value of H for large $|\alpha|$, the kernel in (29) may be expressed as

$$\int_{-\infty}^{+\infty} H(\alpha,x)\, e^{i(t-y)\alpha} d\alpha = \int_{-\infty}^{+\infty} H^{\infty}(\alpha,x)\, e^{i\alpha(t-y)} d\alpha$$

$$+ \int_{-\infty}^{+\infty} [\, H(\alpha,x) - H^{\infty}(\alpha,x)\,]\, e^{i\alpha(t-y)} d\alpha\,, \tag{31}$$

where H^{∞} is the asymptotic value of $H(\alpha,x)$ for $|\alpha| \to \infty$. The first term on the right-hand side of (31) gives a Canchy-type kernel $(t-y)^{-1}$ and the second integral is uniformly converged for all t and y in which the limit $x=0$ can, therefore, be put under the integral sign. After some rather complicated and lengthy manipulations (mostly due to the large number of elastic constants) (29) may be shown to be a singular integral equation with a simple Chachy-type singularity of the following form :

$$\mu_1 \int_L \left[\frac{1}{t-y} + k(y,t)\right] G_1(t)\, dt = p_1(y), \qquad y \in L, \tag{32}$$

where μ_1 is a material constant and

$$K(y,t) = \int_{-\infty}^{+\infty} | H(\alpha) - H^{\infty}(\alpha)| \, e^{i\alpha(t-y)} d\alpha \, . \tag{33}$$

If $c_i < y < d_i$, $(i=1, \ldots ,n)$ defines the cracks along the y axis, from (27) and (28) it follows that (34) must be solved under the following single-valuedness conditions:

$$\int_{c_i}^{d_i} G_1(t) dt = 0 \, . \qquad (i=1, \ldots ,n) \tag{34}$$

For example, if the plate contains a single crack along $(-a,a)$ subjected to uniform bending moment

$$p_1(y) = -M^{\infty}, \tag{35}$$

it is seen that $L=(-a,a)$ and the solution of the integral equation may be expressed as [10]

$$G_1(t) = \frac{H_1(t)}{\sqrt{1-t^2}} . \tag{36}$$

where the unknown function $g_1(t)$ is bounded in $|t| \leq a$.

Defining now

$$\tau = t/a, \qquad s = y/a\,,$$

$$G_1(t) = \frac{h^2}{6}\frac{\sigma_b}{\mu_1} g_1(\tau), \qquad g_1(\tau) = \frac{h_1(\tau)}{\sqrt{1-\tau^2}},$$

$$\sigma_b = \frac{6M^{\infty}}{h^2}, \tag{37}$$

equation (32) may be expressed as

$$\int_{-1}^{1} \frac{g_1(\tau)}{\sqrt{1-\tau^2}} \left[\frac{1}{\tau - s} + k(s,\tau)\right] d\tau = -1, \qquad |s| < 1, \tag{38}$$

subjected to

$$\int_{-1}^{1} \frac{g_1(\tau)}{\sqrt{1-\tau^2}}\, d\tau = 0. \tag{39}$$

In the symmetric bending problem under consideration, the stress intensity factor at a crack tip $y=d_i$ is defined as follows:

$$k_1(z) = \lim_{y \to d_i} \left[2(y - d_i)\right]^{1/2} \sigma_z(0,y,z). \tag{40}$$

Refering to [10] for the procedure, in this single crack case the stress intensity factor ratio defined by

$$k_{bb} = k_1(1/2) / \sigma_b\sqrt{a}, \qquad k_1(z) = \frac{z}{h/2} k_{bb}\sigma_b\sqrt{a}\,, \tag{41}$$

is found to be

$$k_{bb} = -\pi g(1)\,. \tag{42}$$

We must emphasize again that the major difficulty in this problem is that the functions $m_j(\alpha)$ are not known explicitly in terms of (α). Thus we must make use of a numerical technique to obtain $H(\alpha)$ and then, $k(y,t)$.

2.2.2 The Orthopropic Plate under In-Plane Loading

Similarly for the in-plane loading problem we let

$$\Phi(x,y)=\frac{1}{2\pi}\int_{-\infty}^{+\infty}\phi(x,\alpha)e^{-i\alpha y}d\alpha\,. \tag{43}$$

Substituting now from (43) into (13) and considering the symmetry conditions, we obtain:

for materials of type 1

$$\phi(x,\alpha)=\Omega_1(\alpha)\exp(q_3|\alpha|x)+\Omega_2(\alpha)\exp(q_4|\alpha|x),\qquad (x>0) \tag{44.1}$$

where

$$m_1=q_3=-(C_1+\sqrt{C_1^2-C_2^2})^{1/2},$$

$$m_2=q_4=-(C_1-\sqrt{C_1^2-C_2^2})^{1/2}. \tag{44.2}$$

are real roots of the characteristic equation (13.1) and C_1 and C_2 are given by (14).

for materials of type 2

$$\phi(x,\alpha)=[\Omega_1(\alpha)\cos(q_2\alpha x)+\Omega_2(\alpha)\sin(q_2\alpha x)]\exp(q_1|\alpha|x),\qquad (x>0) \tag{45.1}$$

where

$$m_1 = q_1 + i\,q_2 \qquad (q_1 < 0)$$
$$m_2 = q_1 - i\,q_2 \tag{45.2}$$

are complex conjugate roots of the characteristic equation (13.1).

The membrane problem must be solved under the following boundary condition:

$$N_{xy}(0,y) = 0, \tag{46}$$

$$\lim_{x \to 0^+} N_{xx}(0,y) = p_2(y), \qquad y \in L,$$
$$u(0^+,y) = 0, \qquad y \in L'. \tag{47}$$

One of the two unknown functions Ω_1 and Ω_2 may be eliminated by using (46) and the remaining one may then be obtained from the mixed boundary conditions (47). Defining a new unknown function G_2 by

$$\frac{\partial}{\partial y} u(0^+,y) = G_2(y), \tag{48}$$

using the following expressions obtained from (13), (43) and (44) or (45), for materials of type 1

$$\tau_{xy}=\frac{i}{2\pi}\int_{-\infty}^{+\infty}\alpha\,[\,\Omega_1(\alpha)q_3|\alpha|\,\exp(q_3|\alpha|\,x)+\Omega_2(\alpha)q_4|\alpha|\,\exp(q_4|\alpha|\,x)\,]\,e^{-i\alpha y}d\alpha\,,$$

(49.1)

$$\sigma_x=\frac{1}{2\pi}\int_{-\infty}^{+\infty}(-\alpha^2)\,[\,\Omega_1(\alpha)\exp(q_3|\alpha|\,x)+\Omega_2(\alpha)\exp(q_4|\alpha|\,x)\,]\,e^{-i\alpha y}d\alpha\,,$$

for materials of type 2

$$\tau_{xy}=\frac{i}{2\pi}\int_{-\infty}^{+\infty}\alpha\,\{\Omega_1(\alpha)\,[-q_2\,\alpha\sin(q_2\,\alpha\,x)+q_1|\alpha|\cos(q_2\,\alpha\,x)]+\Omega_2(\alpha)\,[\,q_2\,\alpha\cos(q_2\,\alpha\,x)+q_1|\alpha|\sin(q_2\,\alpha\,x)\,]\,\}\exp(q_1\,|\alpha|\,x)\,e^{-i\alpha y}d\alpha\,,$$

(49.2)

$$\sigma_x=\frac{1}{2\pi}\int_{-\infty}^{+\infty}(-\alpha^2)\,[\,\Omega_1(\alpha)\cos(q_2\,\alpha\,x)+\Omega_2(\alpha)\sin(q_2\,\alpha\,x)\,]\,\exp(q_1\,|\alpha|\,x)\,e^{-i\alpha y}d\alpha\,,$$

and noting that

$$\frac{\partial^2 u}{\partial y^2}=S_{66}\frac{\partial\tau_{xy}}{\partial y}-(\,S_{12}\frac{\partial\sigma_x}{\partial x}+S_{22}\frac{\partial\sigma_y}{\partial x}\,)\,,\qquad(50)$$

one may obtain the following integral equation to determine G_2

$$\mu_2 \int_L \frac{G_2(t)}{t-y}\,dt = p_2(y)\,, \qquad (y \in L) \tag{51}$$

where for materials of type 1

$$\mu_2 = \frac{h}{\pi} \frac{1}{S_{22} q_3 q_4 (q_3 + q_4)}. \tag{52.1}$$

for materials of type 2

$$\mu_2 = \frac{h}{\pi} \frac{1}{2\, S_{22}\, q_1 (\, q_1{}^2 + q_2{}^2)}. \tag{52.2}$$

Equation (51) must be solved under the following single-valuedness conditions,

$$\int_{c_i}^{d_i} G_2(y)dy = 0, \qquad (i = 1, 2, \ldots, n)\,. \tag{53}$$

2.3 The line-spring model for surface crack

The most general description of the line-spring model introduced in [1] has been given in [11]. In a plate containing a part-through crack and subjected to membrane and bending loads, the net ligament (the uncracked portion) around the crack would generally have a constraining effect on the crack surface displacement. By approximately representing the net-ligament stress as a membrane load N and a bending moment M and the crack surface displacement due to N and M as an opening δ and a rotation θ, the three-dimensional crack problem could be reduced to a two-dimensional coupled bending-membrane plate

problem. Furthermore, assuming that the relationship between (N,M) and (δ,θ) may be found through the plane strain results obtained from the solution of an edge-notched strip, the pair of functions (δ,θ) and (M,N), then, are determined from the corresponding mixed boundary value problem for a plate having a through crack in which N and M are treated as unknown crack surface loads.

Let the stress intensity factor for the plane strain problem in Fig. (2.b) be given as

$$K(s) = \sqrt{h}\,[\,\sigma\, g_t(s) + m\, g_b(s)\,]\,, \tag{54}$$

$$s(y) = L(y)/h\,, \tag{55}$$

where functious $g_b(s)$ and $g_t(s)$ are called the shape functions for tension and bending, respectively and given as:

$$g_t(s) = \sqrt{\pi s}\sum_{i=1}^{n} AT_i\, s^{2(i-1)}, \tag{56.a}$$

$$g_b(s) = \sqrt{\pi s}\sum_{i=1}^{n} AB_i\, s^{2(i-1)}. \tag{56.b}$$

The coefficients AT_i and AB_i can be found by applying a suitable curve fitting to the results obtained from [12] which are valid for

$0 < L_0/h < 0.8$.

Referring to [13], the strain energy release rate G_1 in an orthotropic medium may be obtained as:

$$G_1 = K_1^2 \left(\frac{b_{11}b_{22}}{2}\right)^{\frac{1}{2}} \left[\left(\frac{b_{22}}{b_{11}}\right)^{\frac{1}{2}} + \frac{2b_{12}+b_{66}}{2b_{11}}\right]^{\frac{1}{2}} = K_1^2 1/\mu_3 \tag{57}$$

where K_1 is the stress intensity factor and the elastic constants b_{ij} are givens by (see equation(1))

$$b_{11} = \frac{S_{33}S_{22} - S_{23}}{S_{22}},$$

$$b_{22} = \frac{S_{11}S_{22} - S_{12}^2}{S_{22}},$$

$$b_{12} = S_{55},$$

$$b_{66} = \frac{S_{13}S_{22} - S_{12}S_{23}}{S_{22}},$$

$$\mu_3 = \left(\frac{b_{11}b_{22}}{2}\right)^{-\frac{1}{2}} \left[\left(\frac{b_{22}}{b_{11}}\right)^{\frac{1}{2}} + \frac{2b_{12}+b_{66}}{2b_{11}}\right]^{-\frac{1}{2}}. \tag{58}$$

Also, the energy available for fracture can be expressed as:

$$G_1 = \frac{\partial}{\partial L}(U - V) = \frac{1}{2}\left(N\frac{\partial \delta}{\partial L} + M\frac{\partial \theta}{\partial L}\right). \tag{59}$$

Combining now (57) and (59) and using (54) we obtain

$$\frac{1}{\mu_3}\left(\sigma^2 g_t^2 + 2\sigma m g_b g_t + m^2 g_b^2\right) = \frac{1}{2}\left[\sigma\frac{\partial}{\partial L}(h\delta) + m\frac{\partial}{\partial L}\left(\frac{h^2\theta}{6}\right)\right]. \tag{60}$$

From (60) it can be shown that

$$\frac{h}{6}\theta = 2h\frac{1}{\mu_3}\left(\alpha_{bb}m + \alpha_{bt}\sigma\right), \tag{61}$$

$$\delta = 2h\frac{1}{\mu_3}\left(\alpha_{tb}m + \alpha_{tt}\sigma\right),$$

where α_{ij} are the compliance coefficients and are given by

$$\alpha_{ij} = \frac{1}{h}\int_0^L g_i g_j dL \ , \qquad (i,j = b,t). \tag{62}$$

From (28) and (48) it may be seen that

$$\theta = 2\phi_x(0,y) = 2\int_{c_i}^{y} G_1(t)dt,$$

$$\delta = 2u(0,y) = 2\int_{c_i}^{y} G_2(t)dt. \tag{63}$$

Solving (61) for σ and m and substituting from (63), we obtain

$$M(y) = \frac{h^2}{6}m = \mu_3\left[\frac{h^2}{36}\gamma_{bb}\int_{c_i}^{y} G_1(t)dt + \frac{h}{6}\gamma_{bt}\int_{c_i}^{y} G_2(t)dt\right],$$

$$N(y) = h\sigma = \mu_3\left[\frac{h}{6}\gamma_{tb}\int_{c_i}^{y} G_1(t)dt + \gamma_{tt}\int_{c_i}^{y} G_2(t)dt\right], \tag{64}$$

$$\gamma_{bb} = \frac{\alpha_{bb}}{\Delta}, \qquad \gamma_{bt} = -\frac{\alpha_{bt}}{\Delta},$$

$$\gamma_{tb} = -\frac{\alpha_{tb}}{\Delta}, \qquad \gamma_{bb} = \frac{\alpha_{tt}}{\Delta},$$

$$\Delta = \alpha_{bb}\alpha_{tt} - \alpha_{bt}^{2}. \tag{65}$$

One should keep in mind that α_{ij}, consequently γ_{ij} are fuctions of $L(y)/y$ and that $L(y)$ describes the surface crack profile.

As an example let us now consider a plate containing a single surface crack, as shown in Fig. 2. By using this model, the crack may be assumed to be a through crack of length 2a and the constraint caused by the net ligament may be accounted for by applying the membrane and bending resultants $N(y)$ and $M(y)$ on the crack surfaces. One may note that these net ligament stresses tend to prevent the crack face from opening and rotating. The mixed boundary condition corresponding to (27) and (47) may be expressed as :

$$\begin{aligned} &M_{xx} = G_1(y) + M(y), && -a < y < a \\ &\phi_x(0,y) = 0, && |y| > a \end{aligned} \tag{66}$$

and

$$N_{xx}(0,y) = G_2(y) + N(y), \qquad -a < y < a \tag{67}$$

$$u(0,y) = 0. \qquad |y| > a$$

The integral equstions, corresponding to (32) and (51) then become :

$$\mu_1 \int_{-a}^{a} [\frac{1}{t-y} + k(y,t)]\, G_1(t)dt = p_1(y) + M(y)\,, \qquad |y| < a \tag{68.a}$$

$$\mu_2 \int_{-a}^{a} [\frac{1}{t-y}]\, G_2(t)\, dt = p_2(y) + N(y)\,, \qquad |y| < a \tag{68.b}$$

where

$$M(y) = \mu_3 \, [\, \frac{h^2}{36} \gamma_{bb} \int_{-a}^{y} G_1(t)\, dt + \frac{h}{6} \gamma_{bt} \int_{-a}^{y} G_2(t)\, dt \,], \tag{68.c}$$

$$N(y) = \mu_3 \, [\, \frac{h}{6} \gamma_{tb} \int_{-a}^{y} G_1(t)\, dt + \gamma_{tt} \int_{-a}^{y} G_2(t)\, dt \,]. \tag{68.d}$$

As seen from (68) in the surface crack problem the integral equation for bending and tension are coupled.

2.4 Two special cases of surface cracks

As mentioned earlier, integral equations for the general case given in (32) and (51) are valid for any number of collinear cracks. But in this study, for the purpose of simplification, we only consider two special cases: a single symmetric crack and two arbitrarily arranged collinear cracks.

In the first case, referring to Fig. 2, assuming the plate subjected to the uniform bending M^{∞} and tension N^{∞} and introducing the following change in variables

$$\tau = \frac{t}{a}\ , \qquad -a < (t,y) < a\ ,$$

$$s = \frac{y}{a}\ , \qquad -1 < (\tau,s) < 1\ ,$$

$$G_i(t) = g_i(\tau)\ , \qquad (i = 1,2)\ , \tag{69}$$

$$k(y,t) = k_1(s,\tau)\ ,$$

from(68), we obtain:

$$\mu_3 \frac{h^2}{36}\gamma_{bb}\, a \int_{-1}^{s} g_1(\tau)d\tau - \mu_1 \int_{-1}^{1} [\frac{1}{\tau - s} + ak_1(s,\tau)]g_1(\tau)d\tau$$

$$+ \mu_3 \frac{h}{6}\gamma_{bt}\, a \int_{-1}^{s} g_2(\tau)d\tau = M^{\infty}\ , \tag{70.a}$$

$$\mu_3 \frac{h}{6}\gamma_{tb}\, a \int_{-1}^{s} g_1(\tau)d\tau - \mu_2 \int_{-1}^{1} \frac{1}{\tau - s} g_2(\tau)d\tau + \mu_3 \gamma_{tt} a \int_{-1}^{s} g_2(\tau)d\tau = N^{\infty}\ . \tag{70.b}$$

It is seen that (70) has a simple Cauchy kernel and hence the solution of the integral equation is of the following form :

$$g_i(\tau) = \frac{h_i(\tau)}{\sqrt{1 - \tau^2}}, \qquad (i = 1,2)\ , \qquad -1 < \tau < 1\ . \tag{71}$$

Equations (70) may be solved numerically by using the quadrature formulas given , for example , in [9], under the additional conditions:

$$\int_{-1}^{1} g_i(\tau)d\tau = 0\ , \qquad (i = 1,2)\ . \tag{72}$$

After solving (70) for g_1 and g_2, the stress and moment resultants M(y), N(y) may be obtained from (64), and the stress intensity factor $K(y)$ along the crack front is then determined from (54).

The configuration and parameters of the second special case are shown in Fig. 3. In this case the unknown functions G_i should be defined separately for cracks (A,B) and (C,D) as:

G_{11} : derivative of the crack surface rotation for the crack (A,B);

G_{21} : derivative of the crack opening displacement for the crack (A,B);

G_{12} : derivative of the crack suface rotation for the crack (C,D);

G_{22} : derivative of the crack opening displacement for the crack (C,D);

also let N(x) and M(x) for these two cracks be defined separately as follows :

$N_1(x)$: N(x) for the crack (A,B);

$N_2(x)$: N(x) for the crack (C,D);

$M_1(x)$: M(x) for the crack (A,B);

$M_2(x)$: M(x) for the crack (C,D).

For crack (A,B) the system equation can then be written as:

$$M_1(y_1) - \mu_1 \int_A^B [\frac{1}{t-y_1} + k(y_1,t)] G_{11}(t)dt$$

$$- \mu_1 \int_C^D [\frac{1}{t-y_1} + k(y_1,t)] G_{12}(t)dt = M^\infty,$$

$$N_1(y_1) - \mu_2 \int_A^B [\frac{1}{t-y_1}] G_{21}(t)dt - \mu_2 \int_C^D \frac{1}{t-y_1} G_{22}(t)dt = N^\infty, \qquad (73)$$

$$A < y_1 < B$$

similarly for crack (C,D) we have

$$M_2(y_2) - \mu_1 \int_A^B [\frac{1}{t-y_2} + k(y_2,t)] G_{11}(t)dt$$

$$- \mu_1 \int_C^D [\frac{1}{t-y_2} + k(y_2,t)] G_{12}(t)dt = M^\infty,$$

$$N_2(y_2) - \mu_2 \int_A^B [\frac{1}{t-y_2}] G_{21}(t)dt - \mu_2 \int_C^D \frac{1}{t-y_2} G_{22}(t)dt = N^\infty, \qquad (74)$$

$$C < y_2 < D$$

where

$$M_i(y) = \mu_3 [\frac{h^2}{36}\gamma_{bb}\int_{c_i}^{y_i} G_{1i}(t)\,dt + \frac{h}{6}\gamma_{bt}\int_{c_i}^{y_i} G_{2i}(t)\,dt],$$

$$N_i(y) = \mu_3 [\frac{h}{6}\gamma_{tb}\int_{c_i}^{y_i} G_{1i}(t)\,dt + \gamma_{tt}\int_{c_i}^{y_i} G_{2i}(t)\,dt]. \qquad (75)$$

Again, we have to convert the limits of integrals to (-1,1) for mumerical solution by introducing the following parameters:

$$t_1 = \frac{B-A}{2}\tau_1 + \frac{B+A}{2} = a\tau_1 + (a + d/2),$$

$$y_1 = \frac{B-A}{2}s_1 + \frac{B+A}{2} = as_1 + (a + d/2),$$

$$t_2 = \frac{D-C}{2}\tau_2 + \frac{D+C}{2} = c\tau_2 + (c + d/2),$$

$$y_2 = \frac{D-C}{2}s_2 + \frac{D+C}{2} = cs_2 + (c + d/2),$$

$$G_{ii}(t_k) = g_{ij}(\tau_k),$$

$$k_{ij}(\tau_i, s_i) = k(t_i, y_i),$$

$$\gamma_{bi}(y) = \lambda_{bi}(s). \qquad (i, j, k = 1,2) \tag{76}$$

Substituting from (75) into (73) and (74) we find

$$a\mu_3 \frac{h^2}{36}\lambda_{bb}\int_{-1}^{s_1} g_{11}(\tau_1)d\tau_1 - \mu_1\int_{-1}^{1}[\frac{1}{\tau_1 - s_1} + a\, k_{11}(\tau_1,s_1)]\, g_{11}(\tau_1)\, d\tau_1$$

$$- \mu_1\int_{-1}^{1} F_1(\tau_2,s_1)\, g_{12}(\tau_2)\, d\tau_2 + a\mu_3\frac{h}{6}\lambda_{bt}\int_{-1}^{s} g_{21}(\tau_1)\, d\tau_1 = M^{\infty}, \qquad (77)$$

$$-1 < s_1 < 1$$

$$a\mu_3 \frac{h}{6}\lambda_{tb}\int_{-1}^{s_1} g_{11}(\tau_1)d\tau_1 - \mu_2\int_{-1}^{1}[\frac{1}{\tau_1 - s_1} g_{21}(\tau_1)d\tau_1$$

$$- \mu_2\int_{-1}^{1} F_2(\tau_2,s_1)\, g_{22}(\tau_2)d\tau_2 + a\mu_3\lambda_{tt}\int_{-1}^{s_1} g_{21}(\tau_1)d\tau_1 = N^{\infty}, \qquad (78)$$

$$-1 < s_1 < 1$$

$$c\mu_3 \frac{h^2}{36}\lambda_{bb}\int_{-1}^{s_2} g_{12}(\tau_2)d\tau_2 - \mu_1\int_{-1}^{1}[\frac{1}{\tau_2 - s_2} + ck_{22}(\tau_2,s_2)]\, g_{12}(\tau_2)d\tau_2$$

$$- \mu_1\int_{-1}^{1} F_3(\tau_1,s_2)\, g_{11}(\tau_1)d\tau_1 + c\,\mu_3\frac{h}{6}\lambda_{bt}\int_{-1}^{s_2} g_{22}(\tau_2)d\tau_2 = M^{\infty}, \qquad (79)$$

$$-1 < s_2 < 1$$

$$c\,\mu_3 \frac{h}{6}\lambda_{tb}\int_{-1}^{s_2} g_{12}(\tau_2)d\tau_2 - \mu_2\int_{-1}^{1}[\frac{1}{\tau_2 - s_2}]\, g_{22}(\tau_2)d\tau_2$$

$$- \mu_2\int_{-1}^{1} F_4(\tau_1,s_2)\, g_{21}(\tau_1)d\tau_1 + c\mu_3\,\lambda_{tt}\int_{-1}^{s_2} g_{22}(\tau_2)d\tau_2 = N^{\infty}, \qquad (80)$$

$$-1 < s_2 < 1$$

where the kernels F_1, F_2, F_3 and F_4 are bounded in the close interval

$$-1 \leq (\tau_i, s_i) \leq -1, \qquad (i=1,2).$$

This problem has four integral equations (77) -(80) with four unknown functions g_{11}, g_{12}, g_{21} and g_{22} which may be solved by using Gass-Chebyshev closed-type quadrature formula under the following single-valuedness conditions :

$$\int_{-1}^{1} g_{ij}(t)dt = 0, \qquad (i,j=1,2). \tag{81}$$

After solving for the unknown functions, the same procedure for single crack may be used for each crack separately in order to find stress intensity factors. It may be observed that if we let $M_i = 0$, $N_i = 0$ or $\gamma_{ij} = 0$, the integral equations (77)-(80) reduce to the system for two collinear through cracks in which the pair of equations corresponding to bending and tension would be uncoupled. One may also observe that as the distance between the two crack tends to infinity, the Fredholm kernels $F_1, \cdots, F_4$ vanish and the integral equations corresponding to cracks (A,B) and (C,D) would again be uncoupled. For through cracks in the latter case one would obtain four uncoupled equations.

2.5 Some remarks on the formulation of the orthotropic plate problem

In the previous section the general problem for an orthotropic plate is formulated. The formulation is given for an orthotropic material which is defined by Hook's law as expressed in (1). Since this is the first attempt to solve this kind problem, it is important to make the following remarks:

1. Unlike the classical orthotropic plate theory, here six rather than four material constants have been used to formulate the plate bending problem: four to describe the in-plane deformations names E_x, E_y, ν_{xy}, and G_{xy}, (in terms of engineering material constants) and two to describe the out-of-plane deformations, namely G_{xz} and G_{yz}. In the classical bending theory G_{xz} and G_{yz} are assumed to be infinite.

2. Making use of the line-spring model in addition to the plate problem, an approximate solution is given for the three dimensional part-through crack problem. To do this the remaining three material coustants E_z, ν_{zx}, ν_{zz} (referring to Fig. 2) have also been introduced to the formulation. Thus, all nine material constants of orthotropy must be specified in order to solve the surface crack problem.

3. As we mentioned earlier, if the plate material is isotropic, instead of one sixth order fundamental equation given by (11), the governing equation may be expressed in terms of one fourth order and one second order differential equation (see, for example [2]). Thus, it is analytically impossible to arrive at the same isotropic plate formulation as given in [2] by taking the limiting case of the orthotropic plate formulation given in this study. However, good agreement is obtained with the result given in [2] by using elastic constants in the numerical solution of the orthotropic plate problem which are nearly the same as the isotropic constants. It may also be noted that if the isotropic material constants are substituted into the characteristic equation (17), as expected the roots turn out to be the same as those found in the isotropic case.

Chapter 3
Results and discussion

The main interest in this study is in evaluating the stress intensity factor in an orthotropic plate. The similar study for the isotropic plate has been considered before in [2] and [10]. However, some basic and additional results for this case have been studied for the purpose of comparison and extension.

The elastic constants of the materials used in the numerical examples are given in Table 1. Material 1 is basically isotropic, and 2 and 3 are laminated composite material. Except for a 90 degree rotation of the axes of orthotropy, Material 2 and 3 are identical. Most of the results obtained are for loading conditions

$$N(y) = N^{\infty}, \qquad M(y) = 0, \qquad (tension)$$

$$M(y) = M^{\infty}, \qquad N(y) = 0. \qquad (bending)$$

The first case that is studied is the plate containing a through crack and two collinear through cracks. Because of the nature of the plate theory used in analysis, the stress intensity factor is a linear function of the thickness coordinate z [see (41)].

Table 8 and Fig. 4 show the effect of the thickness ratio on the stress intensity factor for a single through crack. The result for the isotropic case ($\nu = 0.3$) are the same as that in [10]. It is clearly seen that the orthotropic materials have relatively higher stress intensity factors . This is due to a higher G_{xy} in these orthotropic cases.

Some numerical results obtained for two arbitrarily arranged collinear

through cracks in a plate under uniform bending are shown in Tables 9-14 and Figures 5-6. Tables 9-11 show the interaction between two cracks with the length of one crack varying for Material 1, 2 and 3 and Tables 12-14 show similar results with the plate thickness varying. Tables 15-16 show the results for a plate under uniform tension. As expected for the distance between the two cracks $d \to \infty$ the single crack results are recovered, and the stress intensity factor at the inner tip is always greater than at the outer tip. Figures 5 and 6 clearly show the effect of bending due to the nonsymmetric orientation of the two cracks in the y direction. It is again noted that for the in-plane stretching problem the material orthotropy has no effect on the stress intensity factor for an infinite orthotropic plate containing a single crack or series of collinear cracks.

After through cracks, the part-through crack problem is considered. As noted before, for the application of the line-spring model, the contour of the part-through crack can be any reasonable curve. Elliptic cracks are studied here since it is believed that the ellipse is the closest contour for the actual shape of the crack which may be encountered in practical applications. Thus, crack length for any cross section , referring to Fig. 2(a), is defined by

$$L(y) = L_0\sqrt{1-(y/a)^2}, \qquad -a < y < a,$$

L_0 being the total crack depth at the midsection $(y=0)$.

Tables 17-19 show the stress intensity factor at $y=0$ in an infinite plate containing a single crack under uniform tension and pure bending for Materials 1, 2 and 3 respectively. In these cases, the stress intensity factors are normalized with respect to K^{∞} which is the corresponding value for an edge crack strip under plane strain condition with the same L_0/h ratio [Fig. 2(b)].

Note that the limiting values of these stress intensity factors are

$$K \to 0, \qquad for \quad \frac{a}{h} \to 0,$$
$$K \to K^{\infty}, \qquad for \quad \frac{a}{h} \to \infty.$$

It should be noted in this case that because of crack closure on the compression side, taken separately the bending results are meaningless. However, they may be used by superposition with tension results which are sufficiently large so that the stress intensity factor on both sides of the crack are positive. The coefficients of the shape functions g_b and g_t for these three materials are listed in Tables 3, 5 and 7 which is based on the stress intensity factors shown in Tables 2, 4 and 6.

Figures 7 and 8 clearly show the comparison of different material on the stress intensity factor for L_0/h varying from $0.2 - 0.8$. As expected under bending the crack faces would be closed on the compression side; therefore, for deep cracks the stress intensity factor in an isotropic medium becomes negative. From Tables 18 and 19 and Figures 8 and 9 we have found that the stress intensity factor obtains the negative value as the L_0/h larger than 0.5.

Some results regarding the distribution of the normalized stress intensity factor at the crack front for a single semi-elliptic surface crack are given in Table 20.

The results for two collinear semi-elliptic surface cracks are shown in Tables 21-26. Here the crack profile is defined by

$$L(\bar{y}) = L_0\sqrt{1-\bar{y}^2},$$

$$\bar{y} = \frac{y-(y_B+y_A)/2}{(y_B-y_A)/2} = \frac{y-(B+A)/2}{(B-A)/2}, \qquad A < y < B,$$

$$\bar{y} = \frac{y-(y_D+y_C)/2}{(y_D-y_C)/2} = \frac{y-(D+C)/2}{(D-C)/2}, \qquad C < y < D.$$

Results for the interaction of these two collinear, semi-elliptic surface cracks with the distance between them varying from $d/a = 0.1 - \infty$ and the length of one crack varying from $c/a = 0.1 - 1.$ under tension or bending have been tabulated in Tables 21-23 for material 1, 2 and 3 respectively. The effect of L_0/h on the normalized stress intensity factor for the case of these two collinear cracks has also been considered. Tables 24-26 show this effect for the case of two identical collinear cracks. It may be observed again from all of these tables that the material orthotropy does have significant effect on the fracture parameter for the surface crack.

Finally, an additional example has been given for a crystalline material TOPAZ [Sio_4AL_2 $(F,OH)_2$] which has an orthohomibiz system behavior. The material constants of TOPAZ, given by [14], are as follows:

(unit 10^{-13} cm^2/dyne)

Material 4	S_{11}=4.43	S_{22}=3.53	S_{33}=3.84
	S_{44}=9.25	S_{55}=7.52	S_{66}=7.63
	S_{12}=-1.38	S_{13}=-0.86	S_{23}=-0.66

	S_{11}=3.53	S_{22}=4.43	S_{33}=3.84
Material 5	S_{44}=7.52	S_{55}=9.25	S_{66}=7.63
	S_{12}=-1.38	S_{13}=-0.66	S_{23}=-0.86

Note that the only difference between Material 4 and Material 5 is a 90 degree rotation of orthotropy. Table 27 shows the effect of the thickness ratio a/h on the stress intensity factor in a single through cracked plate under uniform bending for Material 4 and Material 5. and Table 28 shows the effect of L_0/h on the normalized stress intensity factor at the deepest penetration point of a semi-elliptic surface crack under uniform tension and bending moment. It may be seen from these tables that there is no important difference between these two kinds of orthotropy orientations, as this material does not have strong orthotropic material properties.

Tables and Figures

Table 1: Elastic constants of the materials used in the examples

		Mat.1	Mat.2	Mat.3
E_x	psi	$2.2447 \cdot 10^6$	$5.86 \cdot 10^6$	$22.2 \cdot 10^6$
	GPa	15.477	40.405	153.069
E_y	psi	$2.26 \cdot 10^6$	$22.2 \cdot 10^6$	$5.86 \cdot 10^6$
	GPa	15.583	153.069	40.405
E_z	psi	$2.26 \cdot 10^6$	$3.3 \cdot 10^6$	$3.3 \cdot 10^6$
	GPa	15.583	22.754	22.754
G_{xy}	psi	$0.866 \cdot 10^6$	$4.25 \cdot 10^6$	$4.25 \cdot 10^6$
	GPa	5.971	29.304	29.304
G_{yz}	psi	$0.866 \cdot 10^6$	$0.592 \cdot 10^6$	$0.225 \cdot 10^6$
	GPa	5.971	4.082	1.551
G_{xz}	psi	$0.866 \cdot 10^6$	$0.225 \cdot 10^6$	$0.592 \cdot 10^6$
	GPa	5.971	1.551	4.082
ν_{xy}		0.3	0.484	1.834
ν_{yz}		0.3	0.195	0.261
ν_{xz}		0.3	0.261	0.195

Table 2: The coefficients of AT_i and AB_i for the shape functions g_t and g_b (Material 1)

i	AT_i	AB_i
1	1.122	1.120
2	6.520	-1.887
3	-12.388	18.014
4	89.055	-87.385
5	-188.608	241.912
6	207.387	-319.940
7	-32.052	168.011

Table 3: Stress intensity factors in an edge crack under tension (N) or bending (M), (Material 1)

$$\left(\sigma = \frac{N}{h}, \quad m = \frac{6M}{h^2} \right)$$

$\frac{L}{h}$	$\frac{K_N}{\sigma\sqrt{L}}$	$\frac{K_M}{m\sqrt{L}}$
0.001	1.122	1.120
0.1	1.189	1.047
0.2	1.367	1.055
0.3	1.660	1.124
0.4	2.111	1.261
0.5	2.825	1.498
0.6	4.033	1.915
0.7	6.355	2.728
0.8	11.955	4.691

Table 4: The coefficients of AT_i and AB_i for the shape functions g_t and g_b (Material 2)

i	AT_i	AB_i
1	1.047	1.043
2	7.639	-1.610
3	-27.969	17.276
4	175.360	-84.989
5	-439.451	232.556
6	557.540	-304.196
7	-222.80	158.307

Table 5: Stress intensity factors in an edge crack under tension (N) or bending (M), (Material 2)

$$(\sigma=\frac{N}{h},\quad m=\frac{6M}{h^2}\ )$$

$\frac{L}{h}$	$\frac{K_N}{\sigma\sqrt{L}}$	$\frac{K_M}{m\sqrt{L}}$
0.001	1.042	1.041
0.1	1.129	0.992
0.2	1.318	1.013
0.3	1.607	1.083
0.4	2.042	1.211
0.5	2.721	1.430
0.6	3.860	1.814
0.7	6.038	2.563
0.8	11.277	4.372

Table 6: The coefficients of AT_i and AB_i for the shape functions g_t and g_b (Material 3)

i	AT_i	AB_i
1	1.055	1.051
2	7.461	-1.664
3	-25.426	17.517
4	160.659	-85.711
5	-396.808	234.182
6	498.577	-306.252
7	-191.359	159.403

Table 7: Stress intensity factors in an edge crack under tension (N) or bending (M), (Material 3)

($\sigma = \frac{N}{h}$, $m = \frac{6M}{h^2}$)

$\frac{L}{h}$	$\frac{K_N}{\sigma\sqrt{L}}$	$\frac{K_M}{m\sqrt{L}}$
0.001	1.050	1.049
0.1	1.134	0.996
0.2	1.321	1.016
0.3	1.611	1.086
0.4	2.048	1.215
0.5	2.730	1.436
0.6	3.876	1.823
0.7	6.068	2.577
0.8	11.350	4.402

Table 8: The effect of the thickness ratio on the stress intensity factor in a plate under uniform bending, containing a single crack, $\sigma_b = 6M_0/h^2$

	$\frac{a}{h}$	Mat.1	Mat.2	Mat.3
	0.05	0.9885	0.9992	0.9987
	0.1	0.9676	0.9974	0.9957
	0.25	0.8992	0.9886	0.9823
	0.5	0.8195	0.9689	0.9548
$\frac{k_1}{\sigma_b\sqrt{a}}$	1	0.7477	0.9276	0.9050
	2	0.7003	0.8664	0.8434
	4	0.6701	0.8086	0.7942
	6	0.6446	0.7776	0.7657
	10	0.6481	0.7166	0.7044

Table 9: Stress intensity factors in a plate containing two collinear cracks subjected to uniform bending moment M_0 (Material 1)

($a=\frac{B-A}{2}$, $c=\frac{D-C}{2}$, d=C-B, $\frac{a}{h}=1$)

	$\frac{c}{a}$	$\frac{d}{a}\rightarrow$ 0.1	0.25	0.5	1	2	∞
$\frac{k_{1A}}{\sigma\sqrt{a}}$	1	0.8799	0.8551	0.8313	0.8045	0.7798	0.7477
	0.5	0.8071	0.7938	0.7821	0.7698	0.7593	0.7477
	0.25	0.7711	0.7647	0.7598	0.7551	0.7513	0.7477
	0.1	0.7532	0.7512	0.7500	0.7490	0.7482	0.7477
$\frac{k_{1B}}{\sigma\sqrt{a}}$	1	1.294	1.076	0.9599	0.8697	0.8049	0.7477
	0.5	1.063	0.9143	0.8458	0.7995	0.7698	0.7477
	0.25	0.9161	0.8220	0.7863	0.7663	0.7550	0.7477
	0.1	0.8088	0.7678	0.7563	0.7514	0.7489	0.7477
$\frac{k_{1C}}{\sigma\sqrt{a}}$	1	1.294	1.076	0.9599	0.8697	0.8049	0.7477
	0.5	1.012	0.8405	0.7498	0.6786	0.6261	0.5794
	0.25	0.7990	0.6595	0.5867	0.5297	0.4872	0.4496
	0.1	0.5647	0.4577	0.4037	0.3627	0.3325	0.3060
$\frac{k_{1D}}{\sigma\sqrt{a}}$	1	0.8799	0.8551	0.8313	0.8045	0.7798	0.7477
	0.5	0.7395	0.7071	0.6771	0.6434	0.6132	0.5794
	0.25	0.6275	0.5867	0.5507	0.5135	0.4816	0.4496
	0.1	0.4817	0.4293	0.3917	0.3577	0.3308	0.3060

Table 10: Stress intensity factors in a plate containing two collinear cracks subjected to uniform bending moment M_0 (Material 2)

($a=\frac{B-A}{2}$, $c=\frac{D-C}{2}$, d=C-B, $\frac{a}{h}=1$)

	$\frac{c}{a}$	$\frac{d}{a}\rightarrow 0.1$	0.25	0.5	1	2	∞
$\frac{k_{1A}}{\sigma\sqrt{a}}$	1	1.051	1.023	1.001	0.9782	0.9590	0.9276
	0.5	0.9814	0.9658	0.9546	0.9451	0.9373	0.9276
	0.25	0.9488	0.9411	0.9363	0.9328	0.9305	0.9276
	0.1	0.9329	0.9305	0.9293	0.9285	0.9280	0.9276
$\frac{k_{1B}}{\sigma\sqrt{a}}$	1	1.591	1.274	1.122	1.029	0.9773	0.9276
	0.5	1.320	1.106	1.015	0.9665	0.9441	0.9276
	0.25	1.137	1.008	0.9614	0.9405	0.9325	0.9276
	0.1	1.003	0.9500	0.9353	0.9301	0.9284	0.9276
$\frac{k_{1C}}{\sigma\sqrt{a}}$	1	1.591	1.274	1.122	1.029	0.9773	0.9276
	0.5	1.221	0.9665	0.8424	0.7658	0.7240	0.6851
	0.25	0.9261	0.7202	0.6188	0.5567	0.5236	0.4943
	0.1	0.6327	0.4774	0.4023	0.3577	0.3348	0.3154
$\frac{k_{1D}}{\sigma\sqrt{a}}$	1	1.051	1.023	1.001	0.9782	0.9590	0.9276
	0.5	0.8441	0.8019	0.7687	0.7386	0.7151	0.6851
	0.25	0.6817	0.6228	0.5790	0.5436	0.5201	0.4943
	0.1	0.5143	0.4375	0.3880	0.3535	0.3335	0.3154

Table 11: Stress intensity factors in a plate containing two collinear cracks subjected to uniform bending moment M_0 (Material 3)

($a=\frac{B-A}{2}$, $c=\frac{D-C}{2}$, d=C-B, $\frac{a}{h}=1$)

	$\frac{c}{a}$	$\frac{d}{a}\rightarrow 0.1$	0.25	0.5	1	2	∞
$\frac{k_{1A}}{\sigma\sqrt{a}}$	1	1.031	1.004	0.9821	0.9582	0.9375	0.9050
	0.5	0.9595	0.9442	0.9332	0.9238	0.9152	0.9050
	0.25	0.9263	0.9188	0.9141	0.9106	0.9083	0.9050
	0.1	0.9194	0.9080	0.9068	0.9060	0.9059	0.9050
$\frac{k_{1B}}{\sigma\sqrt{a}}$	1	1.547	1.246	1.101	1.011	0.9581	0.9050
	0.5	1.287	1.080	0.9917	0.9452	0.9228	0.9050
	0.25	1.111	0.9841	0.9385	0.9183	0.9103	0.9050
	0.1	0.9103	0.9271	0.9127	0.9076	0.9054	0.9050
$\frac{k_{1C}}{\sigma\sqrt{a}}$	1	1.547	1.246	1.101	1.011	0.9581	0.9050
	0.5	1.206	0.9550	0.8301	0.7507	0.7067	0.6752
	0.25	0.9205	0.7171	0.6150	0.5505	0.5154	0.4912
	0.1	0.6308	0.4775	0.4019	0.3555	0.3311	0.3149
$\frac{k_{1D}}{\sigma\sqrt{a}}$	1	1.031	1.004	0.9821	0.9582	0.9375	0.9050
	0.5	0.8289	0.7869	0.7529	0.7216	0.6981	0.6752
	0.25	0.6777	0.6187	0.5736	0.5364	0.5116	0.4912
	0.1	0.5140	0.4375	0.3872	0.3510	0.3300	0.3149

Table 12: The effect of the thickness ratio on the stress intensity factors under uniform bending moment M_0 (Material 1)

($a=\frac{B-A}{2}$, $c=\frac{D-C}{2}$, d=C-B, $\frac{c}{a}=0.5$)

	$\frac{a}{h}$	$\frac{d}{a}\to 0.1$	0.25	0.5	1	2	∞
$\frac{k_{1A}}{\sigma\sqrt{a}}$	0.5	0.8715	0.8596	0.8502	0.8408	0.8320	0.8195
	1	0.8071	0.7938	0.7821	0.7698	0.7593	0.7477
	2	0.7625	0.7463	0.7322	0.7191	0.7094	0.7003
$\frac{k_{1B}}{\sigma\sqrt{a}}$	0.5	1.148	0.9757	0.9031	0.8631	0.8409	0.8195
	1	1.063	0.9143	0.8458	0.7995	0.7698	0.7477
	2	1.039	0.8898	0.8071	0.7493	0.7184	0.7003
$\frac{k_{1C}}{\sigma\sqrt{a}}$	0.5	1.082	0.8825	0.7872	0.7256	0.6841	0.6358
	1	1.012	0.8405	0.7498	0.6786	0.6261	0.5794
	2	0.9896	0.8147	0.7061	0.6204	0.5675	0.5287
$\frac{k_{1D}}{\sigma\sqrt{a}}$	0.5	0.7831	0.7522	0.7260	0.6989	0.6732	0.6358
	1	0.7395	0.7071	0.6771	0.6434	0.6132	0.5794
	2	0.6933	0.6549	0.6192	0.5837	0.5561	0.5287

Table 13: The effect of the thickness ratio on the stress intensity factors under uniform bending moment M_0 (Material 2)

($a=\frac{B-A}{2}$, $c=\frac{D-C}{2}$, d=C-B, $\frac{c}{a}=0.5$)

	$\frac{a}{h}$	$\frac{d}{a}\to 0.1$	0.25	0.5	1	2	∞
$\frac{k_{1A}}{\sigma\sqrt{a}}$	0.5	1.027	1.009	0.9956	0.9849	0.9772	0.9689
	1	0.9814	0.9658	0.9546	0.9451	0.9373	0.9276
	2	0.9226	0.9087	0.8958	0.8890	0.8865	0.8664
$\frac{k_{1B}}{\sigma\sqrt{a}}$	0.5	1.390	1.160	1.061	1.008	0.9836	0.9689
	1	1.320	1.106	1.015	0.9665	0.9441	0.9276
	2	1.227	1.036	0.9550	0.9100	0.8771	0.8664
$\frac{k_{1C}}{\sigma\sqrt{a}}$	0.5	1.279	1.002	0.8652	0.7796	0.7336	0.6990
	1	1.221	0.9665	0.8424	0.7658	0.7240	0.6851
	2	1.148	0.9248	0.8164	0.7462	0.7024	0.6559
$\frac{k_{1D}}{\sigma\sqrt{a}}$	0.5	0.8692	0.8214	0.7834	0.7495	0.7250	0.6990
	1	0.8441	0.8019	0.7687	0.7386	0.7151	0.6851
	2	0.8144	0.7792	0.7463	0.7204	0.6905	0.6559

Table 14: The effect of the thickness ratio on the stress intensity factors under uniform bending moment M_0 (Material 3)

($a=\frac{B-A}{2}$, $c=\frac{D-C}{2}$, d=C-B, $\frac{c}{a}=0.5$)

	$\frac{a}{h}$	$\frac{d}{a}\to 0.1$	0.25	0.5	1	2	∞
$\frac{k_{1A}}{\sigma\sqrt{a}}$	0.5	1.011	0.9942	0.9817	0.9713	0.9701	0.9548
	1	0.9595	0.9442	0.9332	0.9238	0.9152	0.9050
	2	0.9006	0.8867	0.8720	0.8671	0.8530	0.8433
$\frac{k_{1B}}{\sigma\sqrt{a}}$	0.5	1.371	1.143	1.046	0.9937	0.9638	0.9548
	1	1.287	1.080	0.9917	0.9452	0.9228	0.9050
	2	1.188	1.009	0.9323	0.8880	0.8638	0.8433
$\frac{k_{1C}}{\sigma\sqrt{a}}$	0.5	1.274	1.000	0.8641	0.7773	0.7293	0.6946
	1	1.206	0.9550	0.8301	0.7507	0.7067	0.6752
	2	1.106	0.8840	0.7743	0.7049	0.6668	0.6400
$\frac{k_{1D}}{\sigma\sqrt{a}}$	0.5	0.8671	0.8193	0.7809	0.7460	0.7200	0.6946
	1	0.8289	0.7869	0.7529	0.7216	0.6981	0.6752
	2	0.7688	0.7341	0.7056	0.6791	0.6592	0.6400

Table 15: Stress intensity factors in a plate containing two collinear cracks subjected to uniform tension N_0

$$\left(a=\frac{B-A}{2},\quad c=\frac{D-C}{2},\quad d=C\text{-}B,\quad \frac{a}{h}=1 \right)$$

	$\frac{c}{a}$	$\frac{d}{a}\rightarrow 0.1$	0.25	0.5	1	2	∞
$\frac{k_{1A}}{\sigma\sqrt{a}}$	1	1.151	1.112	1.0811	1.052	1.028	1.000
	0.5	1.066	1.045	1.030	1.018	1.009	1.000
	0.25	1.026	1.016	1.010	1.005	1.003	1.000
	0.1	1.007	1.004	1.002	1.001	1.000	1.000
$\frac{k_{1B}}{\sigma\sqrt{a}}$	1	1.795	1.414	1.229	1.113	1.048	1.000
	0.5	1.449	1.206	1.100	1.043	1.016	1.000
	0.25	1.234	1.090	1.038	1.014	1.005	1.000
	0.1	1.083	1.025	1.009	1.003	1.001	1.000
$\frac{k_{1C}}{\sigma\sqrt{a}}$	1	1.795	1.414	1.229	1.113	1.048	1.000
	0.5	1.329	1.035	0.8889	0.7962	0.7446	0.7071
	0.25	0.9915	0.7595	0.5955	0.5683	0.5280	0.5000
	0.1	0.6732	0.5006	0.4151	0.3624	0.3349	0.3162
$\frac{k_{1D}}{\sigma\sqrt{a}}$	1	1.151	1.112	1.0811	1.052	1.028	1.000
	0.5	0.8956	0.8429	0.8007	0.7626	0.7347	0.7071
	0.25	0.7170	0.6480	0.6425	0.5524	0.5235	0.5000
	0.1	0.5422	0.4557	0.3985	0.3573	0.3336	0.3162

Table 16: The effect of the thickness ratio on the stress intensity factors under uniform tension N_0

($a=\frac{B-A}{2}$, $c=\frac{D-C}{2}$, d=C-B, $\frac{c}{a}=0.5$)

	$\frac{a}{h}$	$\frac{d}{a}\to 0.1$	0.25	0.5	1	2	∞
$\frac{k_{1A}}{\sigma\sqrt{a}}$	0.5	1.066	1.045	1.030	1.018	1.009	1.000
	1	1.066	1.045	1.030	1.018	1.009	1.000
	2	1.066	1.045	1.030	1.018	1.009	1.000
$\frac{k_{1B}}{\sigma\sqrt{a}}$	0.5	1.449	1.206	1.100	1.043	1.016	1.000
	1	1.449	1.206	1.100	1.043	1.016	1.000
	2	1.449	1.206	1.100	1.043	1.016	1.000
$\frac{k_{1C}}{\sigma\sqrt{a}}$	0.5	1.329	1.035	0.8890	0.7962	0.7446	0.7071
	1	1.329	1.035	0.8890	0.7962	0.7446	0.7071
	2	1.329	1.035	0.8890	0.7962	0.7446	0.7071
$\frac{k_{1D}}{\sigma\sqrt{a}}$	0.5	0.896	0.843	0.801	0.763	0.735	0.7071
	1	0.896	0.843	0.801	0.763	0.735	0.7071
	2	0.896	0.843	0.801	0.763	0.735	0.7071

Table 17: Stress intensity factors at the maximum penetration point of a semi-elliptic surface crack in an infinite plate under uniform tension or pure bending (Material 1)

	$\frac{a}{h}$	$\frac{L_0}{h}$ −0.2	0.4	0.6	0.8
$\frac{K_{1b}}{K^{\infty}}$	0.1	0.378	0.060	-0.039	-0.0296
	0.25	0.585	0.184	-0.003	-0.0345
	0.5	0.715	0.309	0.053	-0.0287
	1	0.811	0.446	0.136	-0.0119
	2	0.882	0.586	0.242	0.0179
$\frac{K_{1t}}{K^{\infty}}$	0.1	0.423	0.176	0.079	0.021
	0.25	0.613	0.284	0.124	0.034
	0.5	0.733	0.392	0.176	0.050
	1	0.823	0.510	0.247	0.073
	2	0.889	0.631	0.339	0.104

Table 18: Stress intensity factors at the maximum penetration point of a semi-elliptic surface crack in an infinite plate under uniform tension or pure bending (Material 2)

	$\frac{a}{h}$	$\frac{L_0}{h}$ 0.2	0.4	0.6	0.8
$\frac{K_{1b}}{K^{\infty}}$	0.25	0.518	0.130	-0.025	-0.036
	0.5	0.675	0.255	0.019	-0.036
	1	0.798	0.409	0.097	-0.026
	2	0.873	0.559	0.205	-0.0005
	4	0.924	0.693	0.339	0.045
	6	0.944	0.759	0.425	0.082
	10	0.962	0.829	0.536	0.142
$\frac{K_{1t}}{K^{\infty}}$	0.25	0.552	0.237	0.102	0.027
	0.5	0.697	0.345	0.147	0.039
	1	0.810	0.477	0.215	0.058
	2	0.881	0.608	0.307	0.086
	4	0.928	0.726	0.422	0.129
	6	0.947	0.784	0.496	0.163
	10	0.965	0.846	0.591	0.217

Table 19: Stress intensity factors at the maximum penetration point of a semi-elliptic surface crack in an infinite plate under uniform tension or pure bending (Material 3)

	$\frac{a}{h}$	$\frac{L_0}{h}$ 0.2	0.4	0.6	0.8
$\frac{K_{1b}}{K^{\infty}}$	0.25	0.629	0.212	0.0024	-0.037
	0.5	0.765	0.361	0.069	-0.031
	1	0.861	0.521	0.172	-0.103
	2	0.913	0.660	0.299	0.028
	4	0.948	0.775	0.446	0.090
	6	0.963	0.829	0.534	0.139
	10	0.975	0.882	0.640	0.215
$\frac{K_{1t}}{K^{\infty}}$	0.25	0.654	0.308	0.131	0.035
	0.5	0.780	0.435	0.191	0.051
	1	0.869	0.574	0.279	0.076
	2	0.918	0.696	0.387	0.114
	4	0.952	0.798	0.513	0.170
	6	0.965	0.846	0.589	0.214
	10	0.977	0.894	0.681	0.281

Table 20: Normalized stress intensity factors at the crack front for a semi-elliptic surface crack with $a/h = 1$

		$\frac{y}{a}$	Mat.1	Mat.2	Mat.3
$\frac{L_0}{h} = 0.4$	$\frac{K_{1b}}{K^\infty}$	0.924	0.509	0.498	0.544
		0.707	0.481	0.453	0.538
		0.383	0.450	0.416	0.522
		0.000	0.446	0.409	0.521
	$\frac{K_{1t}}{K^\infty}$	0.924	0.396	0.391	0.419
		0.707	0.453	0.433	0.498
		0.383	0.491	0.461	0.549
		0.000	0.510	0.477	0.574
$\frac{L_0}{h} = 0.6$	$\frac{K_{1b}}{K^\infty}$	0.924	0.275	0.254	0.321
		0.707	0.211	0.183	0.257
		0.383	0.154	0.121	0.195
		0.000	0.136	0.097	0.172
	$\frac{K_{1t}}{K^\infty}$	0.924	0.210	0.200	0.243
		0.707	0.224	0.203	0.258
		0.383	0.239	0.212	0.273
		0.000	0.247	0.215	0.279

Table 21: The interaction between two cracks on the normalized stress intensity factors at the deepst penetration point of a semi-elliptic surface crack under uniform bending or tension (Material 1)

$$a=\frac{B-A}{2},\ c=\frac{D-C}{2},\ d=C-B,\ \frac{a}{h}=1$$
$$y_{0ab}=\frac{B+A}{2},\ y_{0cd}=\frac{D+C}{2},\ \frac{L_o}{h}=0.5$$

	$\frac{c}{a}$	$\frac{d}{a}\to 0.1$	0.25	0.5	1	2	∞
$\frac{K_{0ab}^{(B)}}{K^{\infty}}$	1	0.313	0.306	0.299	0.290	0.283	0.272
	0.5	0.292	0.287	0.282	0.278	0.274	0.272
	0.25	0.280	0.275	0.275	0.273	0.272	0.272
	0.1	0.273	0.273	0.272	0.272	0.272	0.272
$\frac{K_{0cd}^{(B)}}{K^{\infty}}$	1	0.313	0.301	0.299	0.290	0.283	0.272
	0.5	0.197	0.188	0.179	0.171	0.164	0.160
	0.25	0.101	0.091	0.083	0.076	0.072	0.069
	0.1	0.012	0.0045	-0.0004	-0.0038	-0.0057	-0.0058
$\frac{K_{0ab}^{(T)}}{K^{\infty}}$	1	0.397	0.392	0.386	0.379	0.374	0.366
	0.5	0.382	0.378	0.375	0.371	0.368	0.366
	0.25	0.373	0.371	0.369	0.368	0.366	0.366
	0.1	0.367	0.367	0.366	0.366	0.366	0.366
$\frac{K_{0cd}^{(T)}}{K^{\infty}}$	1	0.397	0.392	0.386	0.379	0.374	0.366
	0.5	0.300	0.293	0.286	0.279	0.274	0.269
	0.25	0.217	0.209	0.203	0.198	0.194	0.190
	0.1	0.136	0.130	0.126	0.124	0.124	0.123

Table 22: The interaction between two cracks on the normalized stress intensity factor at the deepst penetration point of a semi-elliptic surface crack under uniform bending or tension

(Material 2)

$$a=\frac{B-A}{2},\ c=\frac{D-C}{2},\ d=C-B,\ \frac{a}{h}=1$$

$$y_{0ab}=\frac{B+A}{2},\ y_{0cd}=\frac{D+C}{2},\ \frac{L_o}{h}=0.4$$

	$\frac{c}{a}$	$\frac{d}{a}\to 0.1$	0.25	0.5	1	2	∞
$\frac{K_{0ab}^{(B)}}{K^{\infty}}$	1	0.444	0.437	0.430	0.423	0.417	0.409
	0.5	0.430	0.425	0.420	0.416	0.412	0.409
	0.25	0.419	0.416	0.414	0.412	0.410	0.409
	0.1	0.412	0.411	0.410	0.410	0.410	0.409
$\frac{K_{0cd}^{(B)}}{K^{\infty}}$	1	0.444	0.437	0.430	0.423	0.417	0.409
	0.5	0.298	0.287	0.277	0.268	0.262	0.255
	0.25	0.171	0.158	0.148	0.140	0.135	0.130
	0.1	0.054	0.043	0.036	0.032	0.029	0.027
$\frac{K_{0ab}^{(T)}}{K^{\infty}}$	1	0.505	0.500	0.494	0.488	0.483	0.477
	0.5	0.494	0.490	0.486	0.482	0.479	0.477
	0.25	0.485	0.482	0.480	0.479	0.478	0.477
	0.1	0.479	0.478	0.477	0.477	0.477	0.477
$\frac{K_{0cd}^{(T)}}{K^{\infty}}$	1	0.505	0.500	0.494	0.488	0.483	0.477
	0.5	0.380	0.370	0.362	0.355	0.350	0.345
	0.25	0.270	0.260	0.252	0.245	0.241	0.237
	0.1	0.168	0.160	0.154	0.150	0.148	0.146

Table 23: The interaction between two cracks on the normalized stress intensity factors at the deepst penetration point of a semi-elliptic surface crack under uniform bending or tension

(Material 3)

$$a=\frac{B-A}{2},\ c=\frac{D-C}{2},\ d=C-B,\ \frac{a}{h}=1$$

$$y_{0ab}=\frac{B+A}{2},\ y_{0cd}=\frac{D+C}{2},\ \frac{L_o}{h}=0.4$$

	$\frac{c}{a}$	$\frac{d}{a}\to 0.1$	0.25	0.5	1	2	∞
$\frac{K_{0ab}^{(B)}}{K^{\infty}}$	1	0.554	0.548	0.542	0.535	0.530	0.522
	0.5	0.542	0.537	0.533	0.529	0.525	0.522
	0.25	0.532	0.529	0.527	0.524	0.523	0.522
	0.1	0.525	0.524	0.523	0.522	0.522	0.522
$\frac{K_{0cd}^{(B)}}{K^{\infty}}$	1	0.554	0.548	0.542	0.535	0.530	0.522
	0.5	0.403	0.393	0.383	0.374	0.367	0.361
	0.25	0.256	0.242	0.231	0.223	0.217	212
	0.1	0.103	0.091	0.083	0.078	0.074	0.072
$\frac{K_{0ab}^{(T)}}{K^{\infty}}$	1	0.600	0.596	0.591	0.585	0.581	0.574
	0.5	0.591	0.587	0.583	0.580	0.577	0.574
	0.25	0.582	0.580	0.578	0.576	0.575	0.574
	0.1	0.576	0.576	0.575	0.575	0.575	0.574
$\frac{K_{0cd}^{(T)}}{K^{\infty}}$	1	0.600	0.596	0.591	0.585	0.581	0.574
	0.5	0.470	0.461	0.453	0.446	0.440	0.435
	0.25	0.343	0.332	0.324	0.316	0.312	0.308
	0.1	0.211	0.202	0.196	0.192	0.189	0.187

Table 24: The effect of L_o/h on the normalized stress intensity factors at the maximum penetration point of two identical collinear semi-elliptic surface cracks under uniform tension or bending (Material 1)

$$y_{0ab}=\frac{B+A}{2},\ a=\frac{B-A}{2},\ d=C-B,\ \frac{a}{c}=1,\ \frac{a}{h}=1$$

	$\frac{d}{a}$	$\frac{L_0}{h}\rightarrow$0.2	0.4	0.5	0.6	0.8
$\frac{K_{0ab}^{(B)}}{K^{\infty}}$	0.1	0.832	0.488	0.313	0.165	-0.005
	0.25	0.829	0.481	0.306	0.159	-0.006
	0.5	0.826	0.470	0.299	0.153	-0.008
	1	0.821	0.465	0.290	0.147	-0.009
	2	0.816	0.456	0.283	0.141	-0.010
	∞	0.811	0.446	0.272	0.135	-0.011
$\frac{K_{0ab}^{(T)}}{K^{\infty}}$	0.1	0.842	0.545	0.397	0.270	0.0755
	0.25	0.840	0.540	0.392	0.266	0.0764
	0.5	0.837	0.533	0.386	0.261	0.0753
	1	0.833	0.526	0.379	0.256	0.0742
	2	0.828	0.518	0.374	0.252	0.0733
	∞	0.823	0.511	0.366	0.247	0.0725

Table 25: The effect of L_o/h on the normalized stress intensity factors at the maximum penetration point of two identical collinear semi-elliptic surface cracks under uniform tension or bending (Material 2)

$$y_{0ab}=\frac{B+A}{2},\ a=\frac{B-A}{2},\ d=C-B,\ \frac{a}{c}=1,\ \frac{a}{h}=1$$

	$\frac{d}{a}$	$\frac{L_0}{h}$ −0.2	0.4	0.6	0.8
$\frac{K_{0ab}^{(B)}}{K^{\infty}}$	0.1	0.815	0.444	0.121	-0.021
	0.25	0.812	0.437	0.115	-0.0224
	0.5	0.809	0.430	0.110	-0.0235
	1	0.806	0.423	0.105	-0.0245
	2	0.802	0.417	0.101	-0.0253
	∞	0.798	0.409	0.097	-0.0260
$\frac{K_{0ab}^{(T)}}{K^{\infty}}$	0.1	0.826	0.505	0.234	0.0622
	0.25	0.823	0.500	0.230	0.0611
	0.5	0.820	0.494	0.226	0.0602
	1	0.817	0.488	0.222	0.0592
	2	0.814	0.483	0.219	0.0585
	∞	0.810	0.477	0.215	0.0578

Table 26: The effect of L_o/h on the normalized stress intensity factors at the maximum penetration point of two identical collinear semi-elliptic surface cracks under uniform tension or bending
(Material 3)

$$y_{0ab}=\frac{B+A}{2},\ a=\frac{B-A}{2},\ d=C-B,\ \frac{a}{c}=1,\ \frac{a}{h}=1$$

	$\frac{d}{a}$	$\frac{L_0}{h}$=0.2	0.4	0.6	0.8
$\frac{K_{0ab}^{(B)}}{K^{\infty}}$	0.1	0.873	0.554	0.201	-0.0026
	0.25	0.871	0.548	0.194	-0.0045
	0.5	0.869	0.542	0.189	-0.0062
	1	0.866	0.535	0.183	-0.0078
	2	0.864	0.530	0.178	-0.009
	∞	0.861	0.522	0.172	-0.0103
$\frac{K_{0ab}^{(T)}}{K^{\infty}}$	0.1	0.880	0.600	0.301	0.0822
	0.25	0.878	0.596	0.297	0.081
	0.5	0.876	0.591	0.292	0.0793
	1	0.874	0.585	0.288	0.080
	2	0.872	0.581	0.283	0.077
	∞	0.869	0.574	0.279	0.076

Table 27: The effect of the thickness ratio on the stress intensity factor in a plate under uniform bending, containing a single crack, $\sigma_b = 6M_0/h^2$ (Material 4 and Material 5)

	$\frac{a}{h}$	Mat.1	Mat.4	Mat.5
$\frac{k_1(h/2)}{\sigma_b\sqrt{a}}$	0.05	0.9885	0.9894	0.9878
	0.125	0.9559	0.9591	0.9536
	0.25	0.8992	0.9059	0.8950
	0.5	0.8195	0.8293	0.8144
	1	0.7477	0.7571	0.7432
	2	0.7003	0.7015	0.6911
	4	0.6701	0.6733	0.6675
	8	0.6521	0.5916	0.5864

Table 28: Stress intensity factors at the maximum penetration point of a semi-elliptic surface crack in an infinite plate under uniform tension or pure bending (Material 4 and Material 5)

		$\frac{a}{h}$	$\frac{L_0}{h}$ →0.2	0.4	0.6	0.8
Mat.4	$\frac{K_{1b}}{K^\infty}$	0.5	0.710	0.303	0.049	-0.029
		1	0.809	0.441	0.130	-0.013
		2	0.872	0.575	0.233	0.015
		4	0.923	0.704	0.365	0.062
		6	0.946	0.776	0.458	0.101
	$\frac{K_{1t}}{K^\infty}$	0.5	0.729	0.387	0.173	0.049
		1	0.820	0.506	0.244	0.071
		2	0.881	0.623	0.332	0.102
		4	0.928	0.736	0.445	0.146
		6	0.949	0.799	0.523	0.182
Mat.5	$\frac{K_{1b}}{K^\infty}$	0.5	0.697	0.290	0.044	-0.0293
		1	0.797	0.424	0.121	-0.0141
		2	0.864	0.558	0.221	0.012
		4	0.918	0.691	0.351	0.057
		6	0.943	0.766	0.444	0.095
	$\frac{K_{1t}}{K^\infty}$	0.5	0.717	0.375	0.169	0.048
		1	0.809	0.491	0.236	0.070
		2	0.873	0.608	0.322	0.099
		4	0.923	0.725	0.433	0.142
		6	0.945	0.790	0.512	0.176

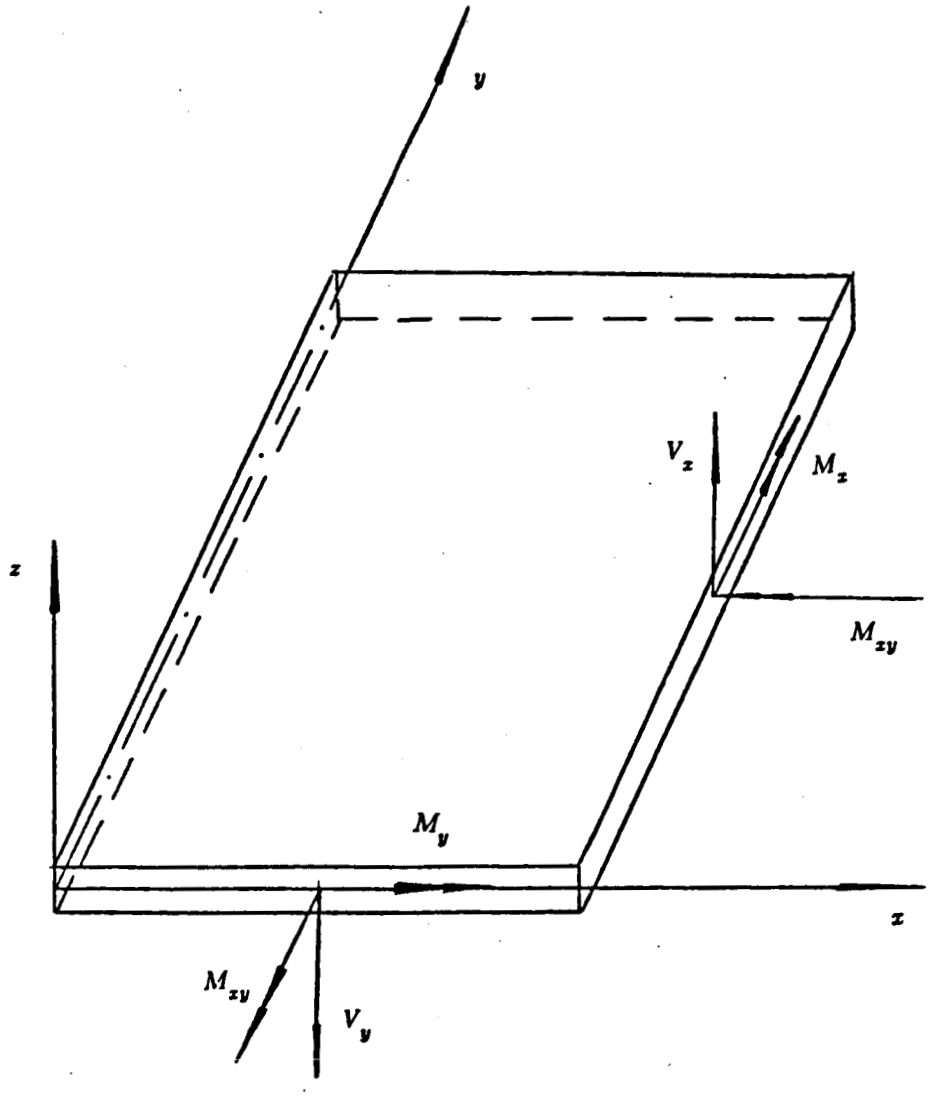

Figure 1: Notation for moment and transverse shear resultants.

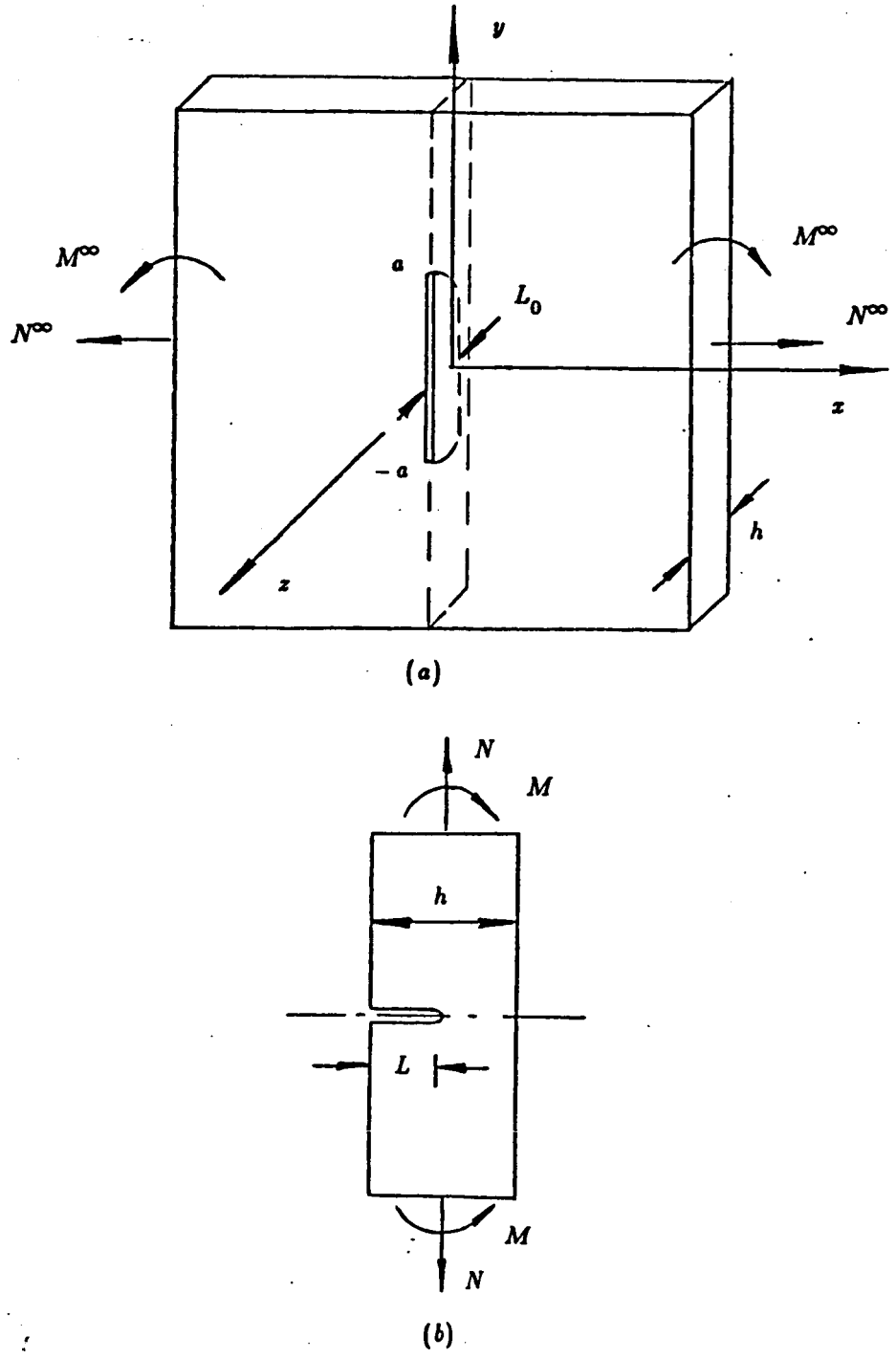

Figure 2: Notation for the part-through surface crack.

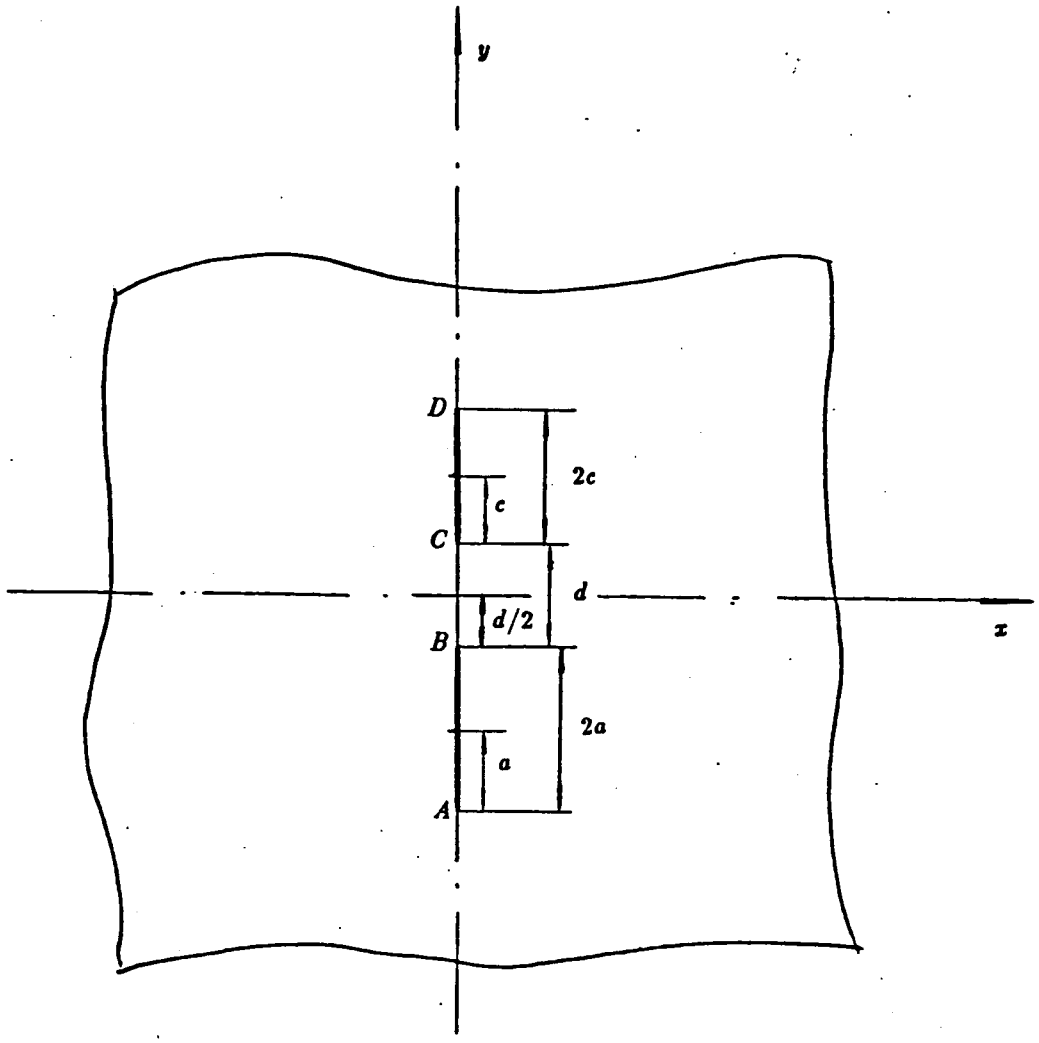

Figure 3: Geometry and notation for two collinear cracks.

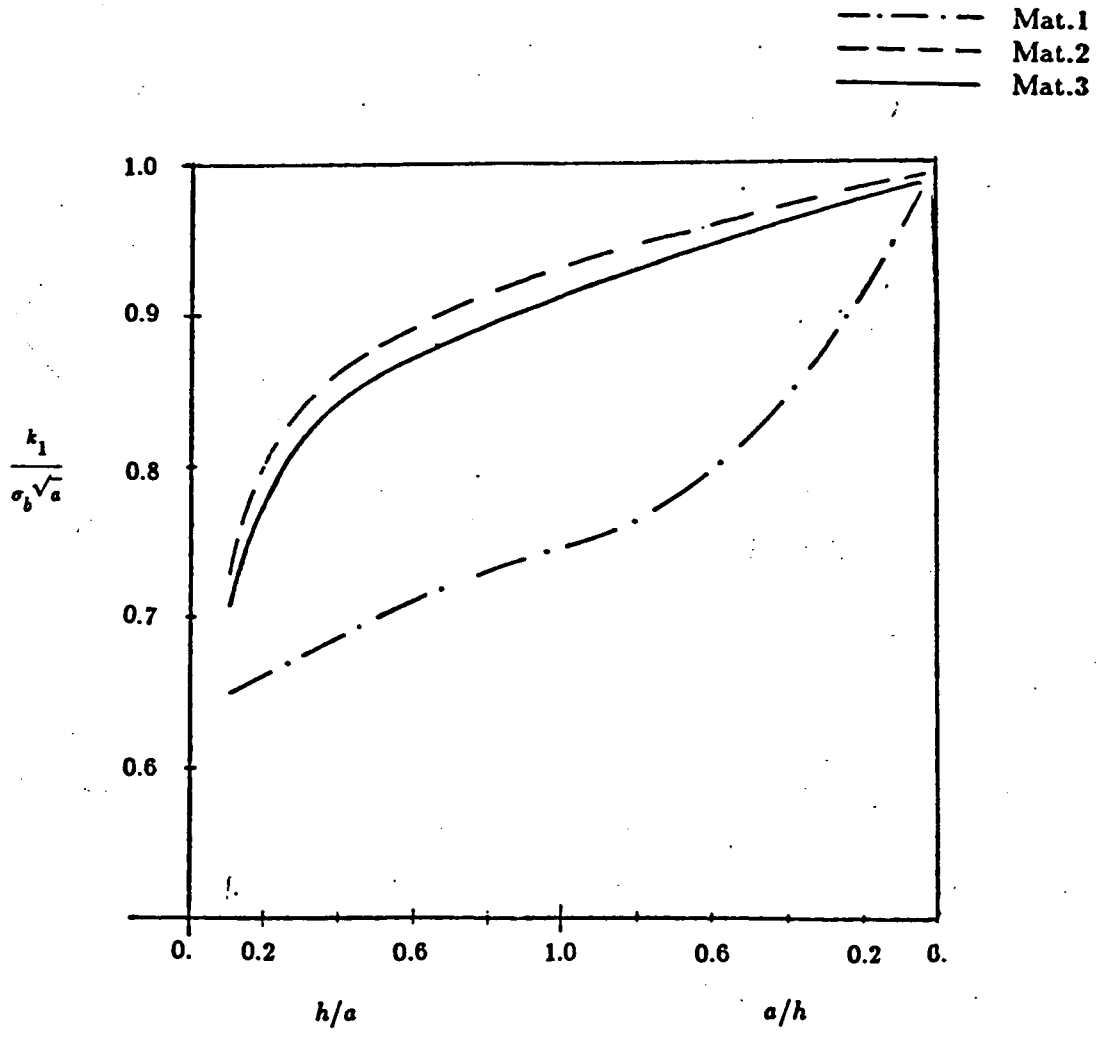

Figure 4: Stress intensity factor in a cracked plate under uniform bending.

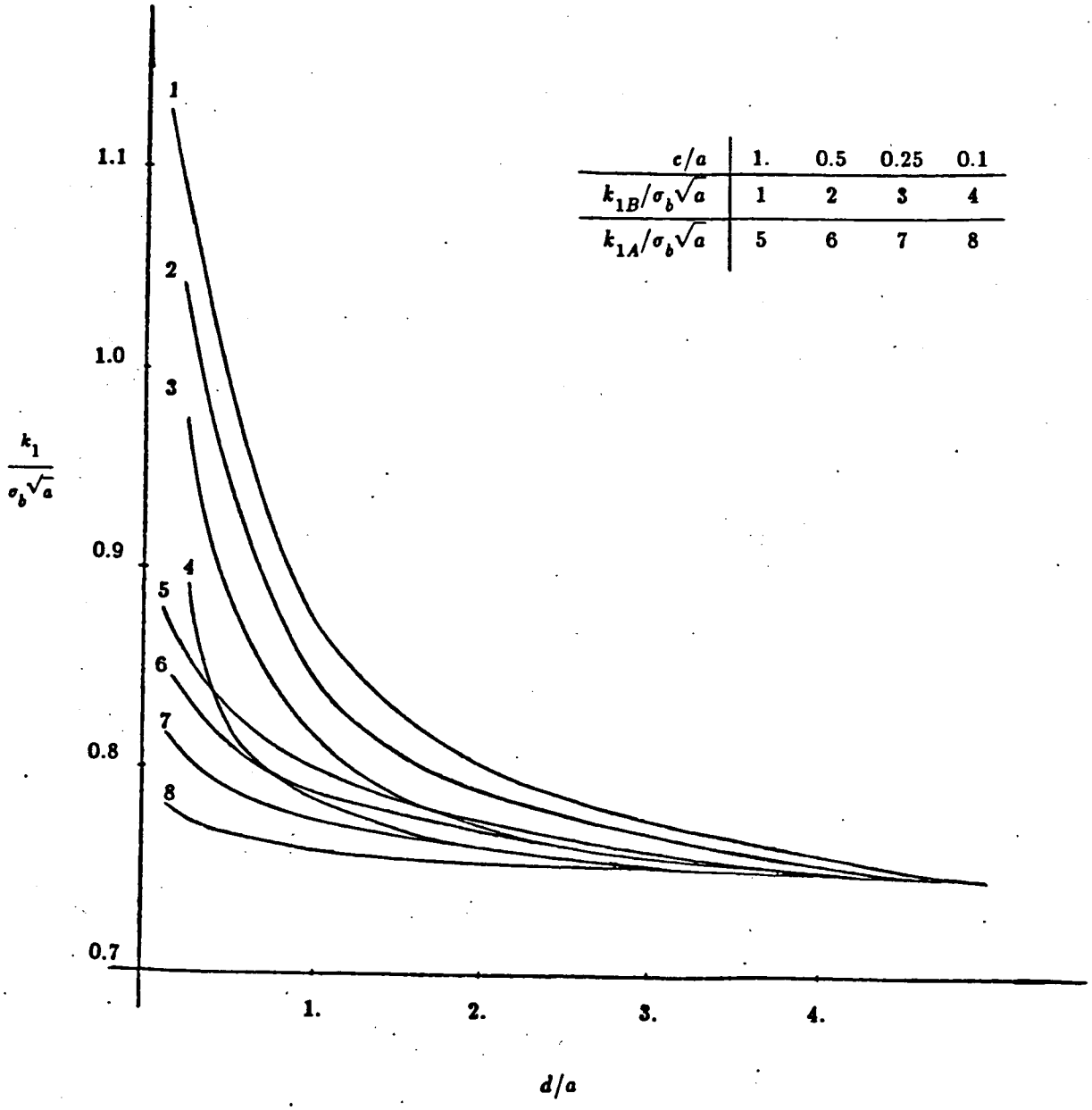

c/a	1.	0.5	0.25	0.1
$k_{1B}/\sigma_b\sqrt{a}$	1	2	3	4
$k_{1A}/\sigma_b\sqrt{a}$	5	6	7	8

Figure 5: Stress intensity factors in a plate containing two collinear through cracks, ($a/h = 1$, Fig. 3, Mat.1).

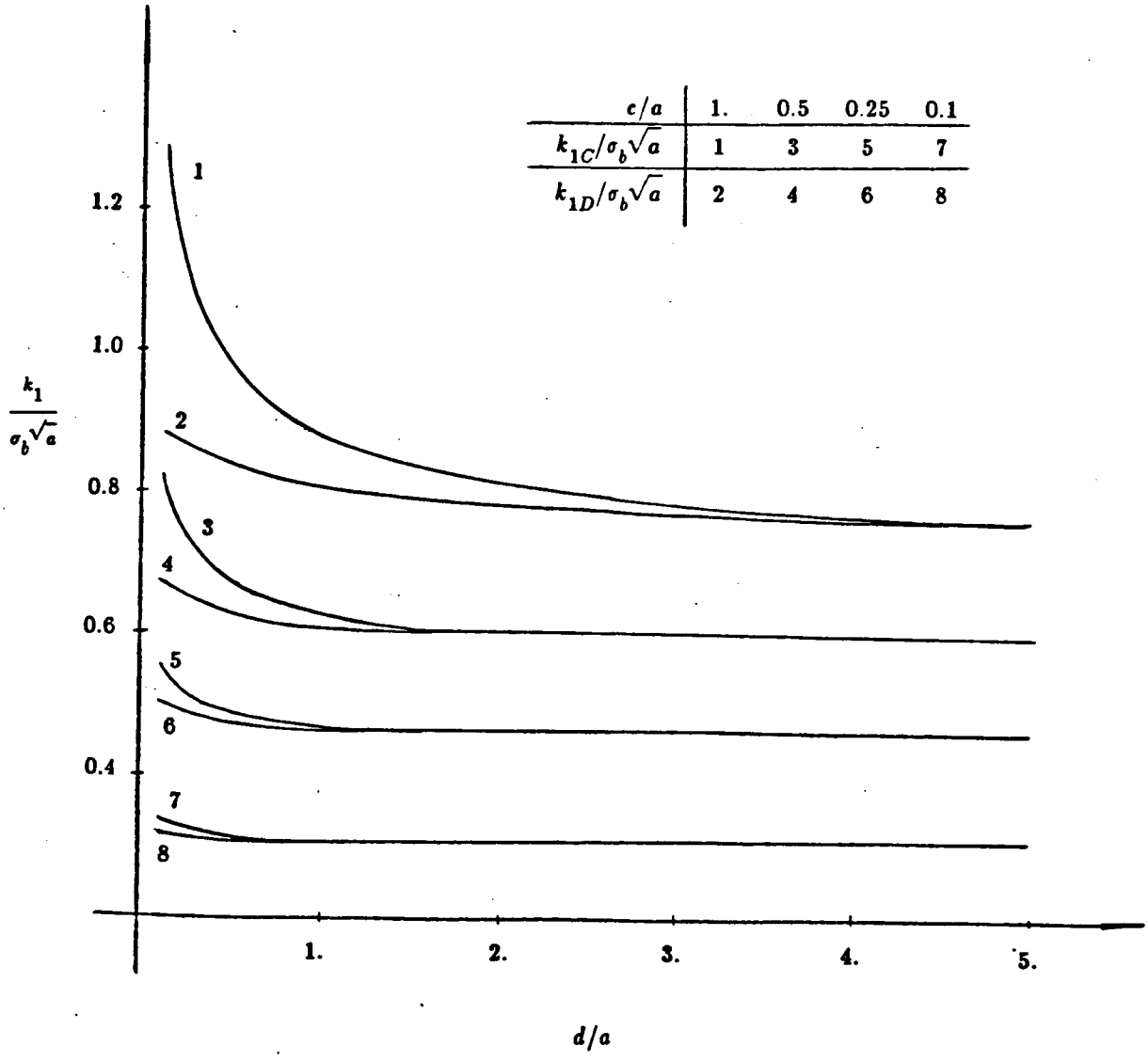

Figure 6: Stress intensity factors in a plate containing two collinear through cracks, ($a/h = 1$, Fig. 3, Mat.1).

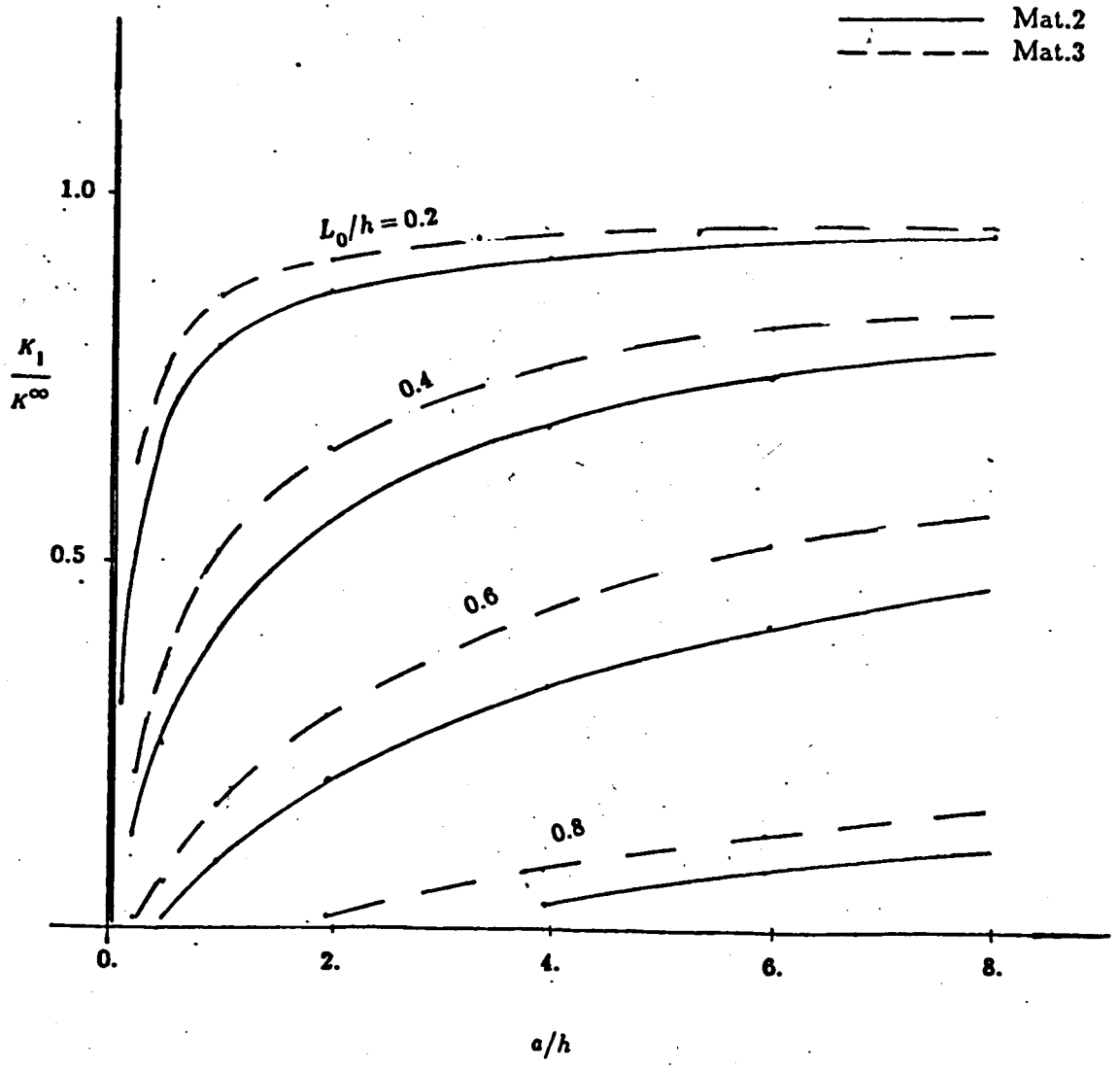

Figure 7: Stress intensity factor at the maximum penetration point of a semi-elliptic surface crack in an infinite plate under pure bending.

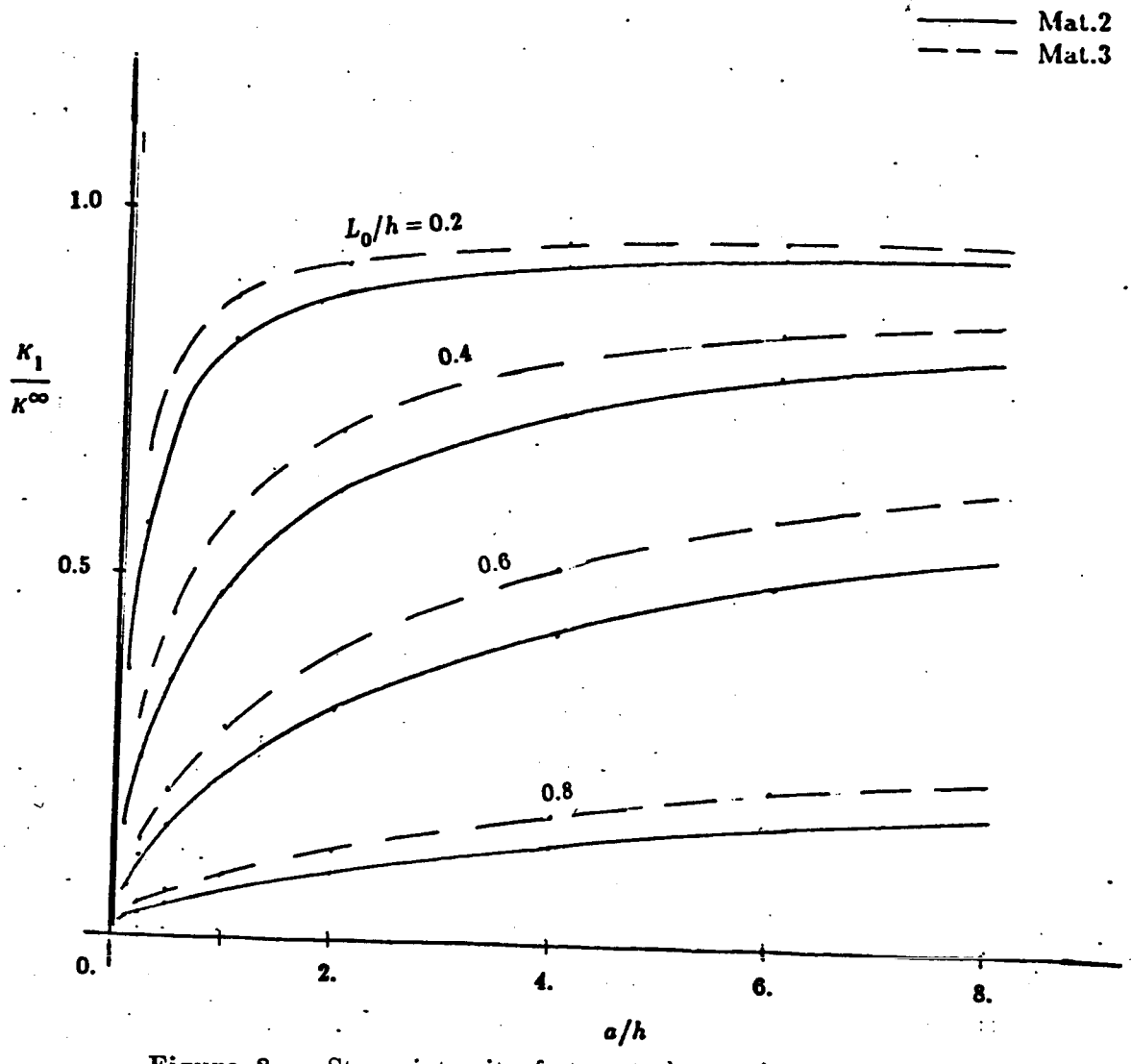

Figure 8: Stress intensity factor at the maximum penetration point of a semi-elliptic surface crack in an infinite plate under uniform tension.

References

1. J.R.Rice and N.Levy, "The part-through crack in an elastic plate", J. Appl. Mech., Vol. 39, Trans. ASME, pp185-194.

2. F.Delale and F.Erdogan, "Line spring model for surface cracks in a Reissner plate", Int. J. Eng. Sci., Vol.19, pp.1331, 1981.

3. F.Erdogan and H.Boduroglu, "Surface cracks in a plate of finite width under extension or bending," Theoretical and Applied Fracture Mechanics, Vol. 1, 1985.

4. F.Erdogan, "Theoretical and experimental study of fracture in pipelines containing circumferential flaws", Final Report under contract DOT-RC-82007, DOT-RSPA-DMA-50/83/3, Sept. 1982

5. E.Reissner, "The effect of transverse shear deformation on the bending of elastic plate", J. Appl. Mech, Vol.12, Trans. ASME ppA69-A77, 1945.

6. E.Reissner, "On bending of elastic plate", Quart. Appl. Math, Vol. 5, pp. 55-68, 1947-1948.

7. S.Timoshenko, "Theory of plate and shells" pp165-171, McGRAW-Hill book company, 1959.

8. S.J.Medwadowski, "A refined theory of elastic, orthotropic plate", J. Appl. Mech, Vol.80, Trans. ASME. pp437-443, 1958.

9. F.Erdogan, "Mixed boundary value problems in mechanics", Mechanics Today, S.Nemat-Nasser, ed., Vol. 4, pp1, Pergamon Press, Oxford, 1978.

10. M.B.Civelek and F.Erdogan, "Elastic-plastic problem for a plate with a part-through crack under extension and bending", Int. J. of Fracture, Vol. 20, pp33-40, 1982.

11. F.Erdogan, "The line spring model", Interim Report, Lehigh University.

12. A.C.Kaya and F.Erdogan, "Stress intensity factors and COD in an orthotropic strip", Int. J. of Fracture, Vol. 16, pp171, 1980.

13. G.C.Sih and Liebowitz, "Mathematical theories of brittle fracture", Fracture - an advanced treatise, H.Liebowitz, ed., Vol. 2, pp110 and 127.

14. R.F.S.Hearmon, "An introduction to applied anisotropic elasticity", Oxford University press, p38, 1961.

Appendix A
Definition of constants A_j and B_j

$$A_1 = -\frac{h^2}{10\kappa}\left(S_{22}S_{55} + S_{12}S_{44} - \kappa\frac{S_{44}}{S_{66}}\right),$$

$$A_2 = -\frac{h^2}{10}\frac{S_{55}}{S_{66}},$$

$$A_3 = -\frac{h^3}{12\kappa}S_{22},$$

$$A_4 = A_7 = -\frac{h^3}{12\kappa}\left(\frac{2\kappa}{S_{66}} - S_{12}\right),$$

$$A_5 = -\frac{h^2 S_{44}}{10 S_{66}},$$

$$A_6 = -\frac{h^2}{10\kappa}\left(S_{11}S_{44} + S_{12}S_{55} - \kappa\frac{S_{55}}{S_{66}}\right),$$

$$A_8 = -\frac{h^3}{12\kappa}S_{11}.$$

$$B_1 = -A_3,$$

$$B_2 = -2A_4,$$

$$B_3 = -A_8,$$

$$B_4 = -A_3A_5,$$

$$B_5 = -A_4A_5 - A_3A_6 - A_1A_4,$$

$$B_6 = -A_4A_6 - A_2A_4 - A_1A_8,$$

$$B_7 = -A_2A_8.$$

Appendix B
Expressions for R_j

(j = 1, 2, 3 for $x > 0$)

$$R_1(\alpha) = \frac{-1}{D(\alpha)} \frac{1}{m_1} (\lambda_3 - \lambda_2) [Q_3\lambda_3\lambda_2 + Q_4(\lambda_3 + \lambda_2)\alpha^2 - Q_5\alpha^2 + Q_6\alpha^4] g_1(t),$$

$$R_2(\alpha) = \frac{-1}{D(\alpha)} \frac{1}{m_2} (\lambda_1 - \lambda_3) [Q_3\lambda_1\lambda_3 + Q_4(\lambda_1 + \lambda_3)\alpha^2 - Q_5\alpha^2 + Q_6\alpha^4] g_1(t),$$

$$R_3(\alpha) = \frac{-1}{D(\alpha)} \frac{1}{m_3} (\lambda_2 - \lambda_1) [Q_3\lambda_1\lambda_2 + Q_4(\lambda_1 + \lambda_2)\alpha^2 - Q_5\alpha^2 + Q_6\alpha^4] g_1(t),$$

where

$$D(\alpha) = (Q_2\alpha^4 + Q_1\alpha^2) [\lambda_2\lambda_3(\lambda_3 - \lambda_2) + \lambda_1\lambda_3(\lambda_1 - \lambda_3) + \lambda_1\lambda_2(\lambda_2 - \lambda_1)],$$

m_i are roots of equation (13) and $\lambda_i = m_i^2$.

$$Q_1 = Q_3 = P_5P_1,$$

$$Q_2 = P_1(P_5P_8 - P_6P_7),$$

$$Q_4 = P_6P_1,$$

$$Q_5 = P_5P_2,$$

$$Q_6 = P_6P_3 - P_5P_4.$$

$$P_1 = \frac{h^5}{120\kappa}\frac{S_{44}}{S_{66}}S_{22},$$

$$P_2 = \frac{h^3}{6}\frac{1}{S_{66}}$$

$$P_3 = -\frac{h^5}{120\kappa}\frac{1}{S_{66}}(S_{22}S_{55} + S_{12}S_{44}),$$

$$P_4 = \frac{h^5}{120\kappa}\frac{S_{55}}{S_{66}}S_{12},$$

$$P_5 = \frac{h^3}{12\kappa}S_{22},$$

$$P_6 = -\frac{h^3}{6}\frac{1}{S_{66}} + \frac{h^3}{12\kappa}S_{12},$$

$$P_7 = -\frac{h^2}{10\kappa}S_{12}S_{44} + \frac{h^2}{10}\frac{S_{44}}{S_{66}},$$

$$P_8 = \frac{h^2}{10\kappa}S_{55}S_{12} - \frac{h^2}{10}\frac{S_{55}}{S_{66}}.$$